A COMPARISON OF FLOW CONTROL STRATEGIES FOR A NOVEL PLAYBACK SMOKING MACHINE

BY

SIMA AZAR

B.E. Electrical Engineering,
American University of Beirut,
Lebanon, July 2002

THESIS

Submitted in Partial Fulfillment of the
Requirements for the Degree of

Master of Science
Electrical Engineering

The University of New Mexico
Albuquerque, New Mexico

May, 2006

Dedication

To my dear family,

and to the love of my life, Raji

Acknowledgements

I would like to thank each of my professors for providing me with distinctive perspectives; Professor Chaouki T. Abdallah for his theoretical insight, Professor Peter Dorato for his never-ending quest for knowledge, and Professor Alan Shihadeh for his valuable understanding of the practical world. I have learned a great deal from you all, and appreciate your support.

To my family, I send love and thanks for believing in me, and for listening to my fear and excitement throughout this expedition of mine.

Thank you to my dearest friends who have been there to hold me up and keep me going when things seem insurmountable.

Last but not least, thank you Raji, for teaching me happiness and love. Thank you for never doubting me and always reminding me of an inner strength. I dedicate my heart and devote my life to you.

A COMPARISON OF FLOW CONTROL STRATEGIES FOR A NOVEL PLAYBACK SMOKING MACHINE

BY

SIMA AZAR

ABSTRACT OF THESIS

Submitted in Partial Fulfillment of the
Requirements for the Degree of

Master of Science
Electrical Engineering

The University of New Mexico
Albuquerque, New Mexico

May, 2006

A COMPARISON OF FLOW CONTROL STRATEGIES FOR A NOVEL PLAYBACK SMOKING MACHINE

by

Sima Azar

B.E., Electrical Engineering, American University of Beirut, 2002

M.S., Electrical Engineering, University of New Mexico, 2004

ABSTRACT

Smoke aerosol toxicology studies are usually conducted by using an instrument that will puff a cigarette or a smoking device such as the narghile waterpipe. ISO and FTC standards for cigarette testing model a person's smoking behavior by a periodic puffing regime; however, studies show that these standards do not produce accurate measurements of a smoker's intake.

The need for a better method to quantify the damaging effects of tobacco smoke has prompted the development of a smoking machine that can reproduce real smoking patterns recorded from an actual smoker. We have built such a machine primarily for the narghile, although it may be modified to accommodate the lower flow rates required in cigarette testing.

This thesis explores two possible control strategies to reproduce real smoking patterns. The first is a feedback linearizing controller derived from an analytical model of the system, while the second controller takes on a more practical approach and employs an adaptive lookup table. One of the challenges is to maintain tracking while collection filters load with particulate matter, which causes the system dynamics to change. Total drawn volume as well as average error in puff volume and the tracking error dynamics were compared using the two approaches. Various scenarios were examined for the filter loading effects.

Contents

List of Figures

Chapter 1

Introduction

As the tobacco industry grows and attracts an increasing number of smokers, toxicology researchers are looking for better ways to quantify the damaging components of tobacco smoke. The development of a "smoking machine" allowed researchers to perform tests without having subjects smoking in the laboratory. It also drove researchers and government authorities to create a standardized protocol by which tobacco smoke can be analyzed. In recent years however, studies have shown that these machines and testing protocols do not adequately represent the true contents of tobacco smoke.

The purpose of this thesis is to design and build a smoking machine that can reproduce "real" smoking behavior, which from a controls perspective, translates to trajectory tracking using flow control. We design and test two controllers implemented using two different approaches, one theoretical and the other experimental.

1.1 Motivation

Smoke aerosol toxicology studies are usually conducted by using an instrument that will puff a cigarette, or a smoking device such as the narghile, also referred to as a water pipe or hookah. These "smoking machines" model a person's smoking behavior by a periodic puffing regime, in compliance with the standard smoking protocol set by the International Organization for Standardization (ISO) and the US Federal Trade Commission (FTC) [9]. In recent years, these standards have been harshly criticized for their inability to produce accurate measurements of the smoker's intake [4].

For instance, cigarette smokers tend to show an effect known as compensation whereby they adjust their smoking behavior according to the availability of nicotine in a particular type of cigarette. Among others, this effect is not reflected in any standardized smoking protocol, and as a result, the World Health Organization (WHO) has urged ISO to "ensure that its members recognize and adhere to the principle that ISO/FTC measurements and methods are used to monitor performance and not health impacts of tobacco products" [14].

Smoking behavior also varies throughout the lifetime of a cigarette, as smokers take shorter puffs and wait longer between puffs towards the end [3]. This effect would be overlooked by the averaged periodic puffing regime. Studies have found that tar and nicotine in cigarettes as measured by current smoking machines are greatly underestimated in comparison with measurements made from the smoker's saliva [5].

This leads to misconceptions about the true contents of cigarette smoke and their amounts when measured with smoking machines. Clearly, there is a need for better methods for quantifying harmful components in tobacco smoke.

Apart from cigarettes, smoking devices such as the narghile also produce significant amounts of toxins, and although limited work has been done to investigate the smoke aerosols it generates, research is beginning to expose the contents of nargileh smoke [11], [10]. The narghile is found primarily in the Middle East, but has been gaining prevalence in Europe and North America, particularly among the younger population. In the US, "hookah lounges" can be found near 45% of colleges and universities [13].

1.2 Objective

The work presented here considers as a main application the development of a smoking machine for the study of smoke aerosols from a narghile. Nonetheless, it may be extended to accommodate other smoking devices or cigarettes. This smoking machine can accurately reproduce recorded smoking sessions any number of times without the continuous presence of the smoker, hence providing an unobtrusive setup for smoke analysis. Smoking sessions are first recorded, which requires a small modification of the narghile hose to incorporate a flow sensor that is discretely connected to a data logger. Most people eventually overlook these modifications since recording is carried out in natural settings such as a café, and the topography recording unit is hidden away from sight. Once the sessions have been recorded, they can be reproduced in the laboratory for a true representation of the smoker's puffing behavior, as opposed to an averaged

parameterization. It would be worthwhile to compare the results in [5] with measurements generated from a more realistic smoking machine.

Having a smoking machine that can reproduce smoking patterns in the laboratory has a number of advantages besides producing a proper representation of the smoker; the machine allows repeatability of the smoking sessions. It also allows the use of "fresh smoke" by minimizing the possible alteration of the volatile smoke sample [3].

Another application of smoking machines is in inhalation exposure studies. For example, the machine may be used to reproduce human breathing patterns to quantitatively study the inhalation of a certain chemical, without repeatedly subjecting the human directly to that chemical.

Looking broadly at the smoking machine, the overall aim is flow control. The low level objective is to control the flow through a system in order to track a desired flow trajectory. While this can be done in an open-loop fashion, closed-loop control infuses some degree of intelligence and robustness, but also becomes necessary when the system characteristics change. In our case, the time-varying component is essentially the loading of the collection filters used to analyze the smoke's contents. As the filters collect particulate matter, flow resistance in the system increases and must be compensated for in order to maintain the desired flowrate.

In this thesis, we develop and compare two different strategies to tackle the challenges of flow control in a time-varying nonlinear system. The first approach models the components of the smoking machine based on fluid dynamics first principles. For the resulting system, we develop a linearizing feedback controller equipped with trajectory tracking. The second control strategy takes on a more practical approach. We design an intelligent adaptive lookup table controller that can be calibrated to any experimental setup on-the-fly. While the two strategies are on either end of the "theoretical vs. practical" spectrum, each presents new insight into understanding the nature of the problem.

1.3 Methodology

For many control problems, there may be more than one solution. Finding the "right" controller requires consideration of the performance, complexity and cost of its implementation.

We will begin by building the smoking machine with careful consideration to practical issues, such as flow and pressure requirements. We will then develop the two controllers and explore their behavior under different scenarios by looking at their performance and practicality for the application at hand.

The comparison will be made based on an implementation of the adaptive lookup table approach and a simulation of the feedback linearizing controller and system model. Each controller will be put to the test under varying system parameters and reference inputs.

The most important performance measure is how well the controllers can track the reference trajectories, indicated by the error in the total volume that has flown through the system, the average error in puff volume, and how quickly the tracking error converges to zero.

1.4 Conclusion

In this chapter, we described current smoke aerosol testing methods and their limitations, and highlighted the need for a new generation smoking machine that can reproduce real smoking patterns. The following chapter provides a detailed account of the hardware components of the smoking machine.

Chapter 2

Smoking Machine Description

2.1 Smoking Machine Hardware Components

The smoking machine consists of a vacuum pump, a proportional valve, a flow sensor, a solenoid valve, filters, and a data acquisition card connected to a computer. The setup is illustrated in Figure 1.

The vacuum pump is set to a constant flowrate, usually the maximum possible, as the flow control is done by adjusting the opening of the proportional valve. We are using the Robinair 15434 vacuum pump, which has a free air displacement of 4 cubic feet per minute (CFM), equivalent to 113 liters per minute (LPM). It employs a rotary vane motor that delivers a vacuum capacity much higher than what our task calls for, in order to ensure a steady and constant flow at all times. A vacuum pump that is not sufficiently powerful will not create a large enough pressure drop, and will have decreased performance as the load increases.

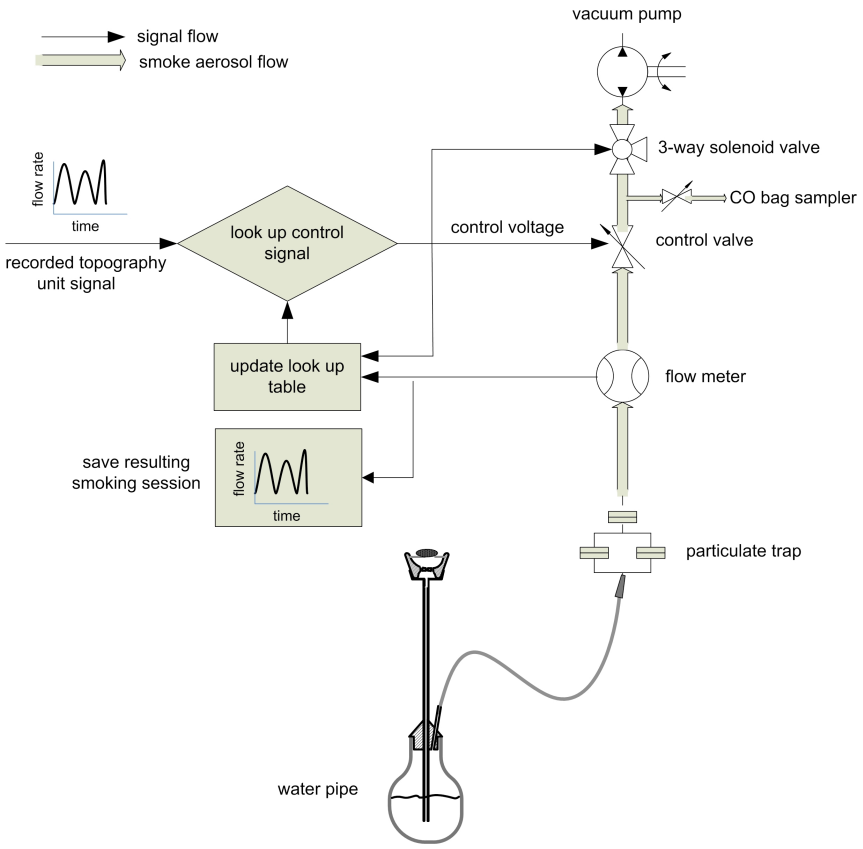

Figure 1 – Schematic of the smoking machine.

While the pump is kept at a constant flowrate, a rapid response 2-way proportional valve receives DC voltage signals from the computer via the data acquisition card to control the flow through the system. The Omega PV104 proportional valve has a 20 ms transition time from fully closed to fully open, and a control signal range of 0-5 VDC. Figure 2 shows the valve's characteristic curve according to the datasheet. The zero offset point, where flow begins, is said to typically be between 30-40% of the control signal. The two curves are the valve characteristics depending on the actual system pressure.

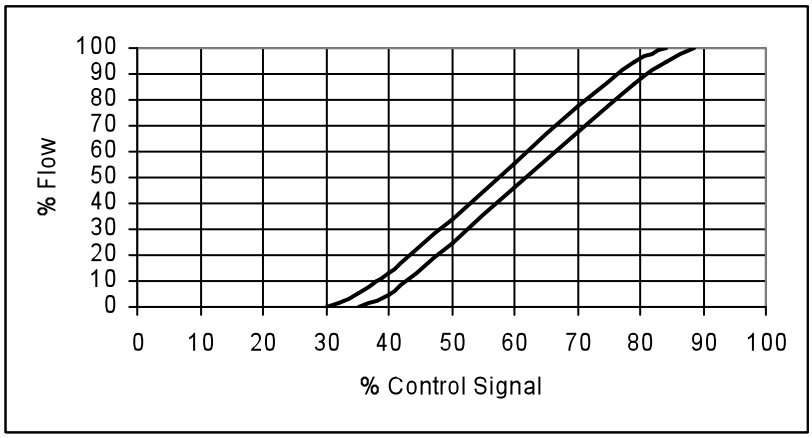

Figure 2 – Flow vs. control signal characteristic curve for the Omega PV104 proportional valve. Linear operating range is approximately within 15-85% of full flow. (Source: Omega PV100 Series Instruction Sheet, M2160/0495)

To protect the pump and the other components when the proportional valve is fully closed, a 3-way solenoid valve diverts the flow from the pump to the rest of the system during a puff, and from the pump to the atmosphere between puffs.

Flowrates are measured using a Honeywell AWM5104 mass airflow sensor, which can read up to 20 LPM, a satisfactory limit for this application. Of course, larger flow sensors may be used just as well. The AWM5104 flow sensor has a maximum response time of 60 ms, and notably linear characteristics as shown in Figure 3. The slope is 0.2 V/LPM, and there is an ideal baseline voltage of 1 V. The measured baseline voltage for this flow sensor is actually 1.24 V, leading to the following flow-voltage relationship

$$\dot{m} = 5(v_f - 1.24) \tag{1}$$

where v_f is the voltage read from the flow sensor output.

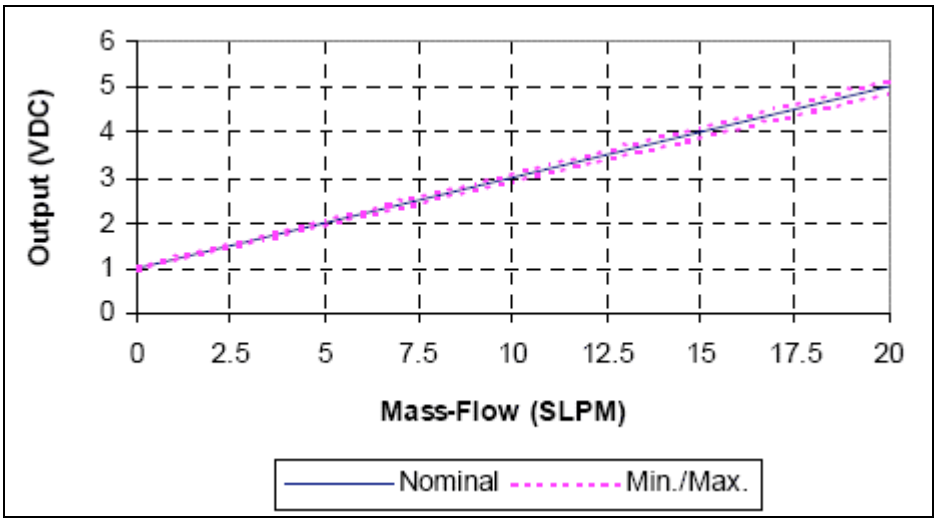

Figure 3 – Honeywell AWM5104 flow sensor voltage-flow characteristics, a linear relationship. (Source: Installation Instructions for the Honeywell AWM5000 Series Microbridge Mass Airflow Sensor, Issue 3, PK 88762)

The flow sensor feeds back the actual flowrate at each time step so that it can be compared with the desired flowrate. Before measurements are made, the flow sensor is given a small buffer time within each sampling interval until a steady reading can be taken.

The smoking machine computer interface and controller algorithm is coded entirely in the National Instruments™ LabVIEW graphical programming language, and communicates with the hardware via the NI-DAQ USB 6009 data acquisition box. As its name suggests, this DAQ uses the computer's USB port, and has a sampling rate of 49,000 samples per second with 16-bit resolution. If a higher sampling frequency is required, other DAQs may be used, although they are usually inserted directly into an expansion slot on the computer's motherboard as opposed to being connected via the USB port. The USB 6009

has 8 Analog Inputs (0-10 VDC), when used in reference single-ended configurations, and 2 Analog Outputs (0-5 VDC). It has a maximum driving current of 50 mA, which is insufficient for the valve and flow sensor, and so an external power supply is used for those devices.

The collection filters can be arranged in different configurations. They are usually laid out in such a way that they do not cause a large pressure drop in the system, and so that particulate matter can be collected on a number of filters for various tests to be performed after the experiment. It is also possible to connect other sampling devices, such as an outlet for carbon monoxide sampling bags, shown in Figure 1.

2.2 Conclusion

This chapter illustrated the major hardware components of the smoking machine. The various specifications needed for performance were explained. In the following chapter, an analytical model of these components is derived based on concepts from fluid dynamics, and a feedback linearizing trajectory tracking controller is designed.

Chapter 3

Nonlinear Model of the Smoking Machine

In this chapter, we derive a first-principles nonlinear model and the first of our two flow control strategies. Using first principle fluid dynamics, we develop a theoretical model of the smoking machine. We start by studying the basic individual components of the machine, in order to combine their descriptions into an inclusive model for the entire system.

The smoking machine has four basic components; collection filters, tubing, a control valve, and a vacuum pump, shown in Figure 4.

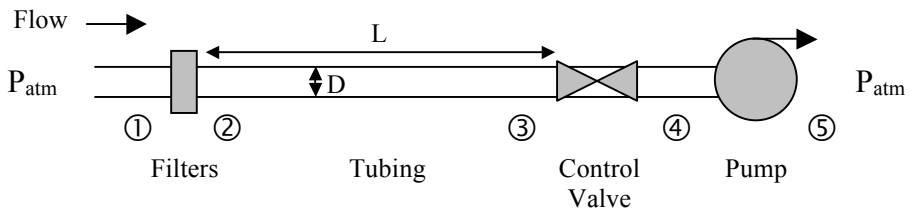

Figure 4 – The smoking machine can be broken down into the basic parts shown here.

Our modeling begins with equations describing the pressure drops across each component. Notice that the flow sensor has not been included here because it is assumed, per its function, to create an insignificant pressure drop across its terminals.

3.1 Modeling the Components

3.1.1 Filters

The pressure drop across the filters can be modeled as a "minor loss" in terms of fluid mechanics. Minor loss, usually given as a coefficient K, is a ratio of head loss to velocity head. Head is defined as the amount of energy a fluid possesses per unit weight [1].

$$K = \frac{\Delta P / \rho g}{V^2 / 2g}$$

$$\Rightarrow \Delta P = \frac{1}{2} \rho K V^2$$

$$= \rho K' V^2$$

where ΔP is the pressure difference across two points

ρ is the density of the air

V is the average velocity of the air

g is the gravitational acceleration.

In this system, K is time-varying, since the filters are loading with time. Although it is possible to derive this loss coefficient empirically, it would be different for each type of filter and for each filter arrangement used. Some experiments call for a number of filters to be placed in parallel to maximize collection sampling. In fact, the theory of minor

losses through fittings and orifices is not developed, and the loss coefficients are usually measured experimentally [12].

The pressure drop across the filters is

$$\Delta P = P_1 - P_2 = \rho K_f(t) V_f^{\,2}$$

Let $P_1 = P_{atm}$,

$$P_2 = P_{atm} - \rho K_f(t) V_f^{\,2} \tag{2}$$

The flow coefficient, K_f, depends on a number of factors including the volume of air flowing through the system, the type of particulate composition of the flow, and naturally, the filter material itself. This is a rather complex and variable relationship for modeling. Alternatively, one could measure the pressure drop across the filter and determine its flow coefficient experimentally.

3.1.2 Tubing

The flow of a fluid through a pipe can be described using the modified Bernoulli equation, which relates pressure, velocity, and elevation. It is derived from the conservation-of-mass and the conservation-of-momentum requirements for a particular control volume [12]. Bernoulli's equation for unsteady laminar (non-turbulent) flow through any two points 1 and 2 of a pipe is

$$\int_1^2 \frac{\partial V}{\partial t} ds + \int_1^2 \frac{dp}{\rho} + f\frac{LV^2}{2D} + \frac{1}{2}(V_2^{\,2} - V_1^{\,2}) + g(z_2 - z_1) = 0 \tag{3}$$

where V is the average velocity of the air

$V_{1,2}$ are the velocities of the air at points 1 and 2, respectively

$z_{1,2}$ is the elevation of the pipe at points 1 and 2, respectively

D is the diameter of the pipe

ds is a small length of pipe.

The first integral represents the unsteadiness of the flow, in that the velocity profile changes with respect to time. For steady flow, $\partial V / \partial t = 0$. It can be interpreted as the inertia within the flow. The procedure for evaluating the second integral depends on whether the fluid is either compressible or incompressible. For an incompressible fluid, the density ρ is constant throughout the pipe. The third term represents frictional losses, or lost head in the flow, which is proportional to a dimensionless parameter, *f*, called the Darcy friction factor. The term involving gravity takes into account losses due to a height difference between those two points along the pipe.

In this problem, the flow is assumed unsteady, the fluid incompressible, and the height difference negligible between points 2 and 3 of Figure 4. We are also assuming that the pipe length between the valve and the pump is negligible, or alternatively has been lumped into the length between the filters and the valve.

The conservation-of-mass requirement states that the mass flow rates at the two points, $\dot{m}_2$ and $\dot{m}_3$ respectively, must be equal. The mass flowrate is related to the velocity by the relationship $\dot{m} = \rho V A$. Then, $\rho V_2 A_2 = \rho V_3 A_3 \Rightarrow V_2 A_2 = V_3 A_3$.

We are also assuming that the entire system has the same cross-sectional area; therefore the velocity is time-varying but the same throughout the length of the tube at any given time. The velocity V is then a function of time only.

$$\int_2^3 \frac{\partial V}{\partial t} ds = \frac{dV}{dt} \int_2^3 ds = L \frac{dV}{dt}$$

where, L is the length of the tube between points 2 and 3, and $V_2 = V_3 = V_f = V$.

We can now write a more specific Bernoulli equation for the pipe length between the filters and the control valve

$$L \frac{dV}{dt} + \frac{P_3 - P_2}{\rho} + f \frac{LV^2}{2D} = 0 \tag{4}$$

The friction factor *f* for laminar flow in a circular pipe is

$$f = \frac{64}{Re}$$

where *Re* is the Reynolds number, which represents a ratio of inertial to viscous or damping forces [8].

$$Re = \frac{\rho VD}{\mu}$$

where μ is the viscosity of air.

The Reynolds number distinguishes between laminar and turbulent flow. If it is less than 2000, the flow is laminar, while a Reynolds number greater than 4000 represents turbulent flow. Between 2000 and 4000, is a transition regime where it is unclear whether

the flow is laminar or turbulent, and may in fact be a mixture of the two. The flow we are dealing with is clearly laminar.

We can now obtain an expression for P_3 by substituting the expressions previously obtained for P_2 and f in Equation (4).

$$P_3 = P_{atm} - \rho K_f(t)V^2 - \rho L\frac{dV}{dt} - \frac{32\mu LV}{D^2} \tag{5}$$

3.1.3 Proportional Valve

Although not necessarily small, the pressure drop across a valve can be modeled as a minor loss. The loss coefficient K_v may be obtained experimentally relative to the state of the valve (fully open, partially open, or closed). This data is usually provided by the manufacturer, as it depends on the valve's mechanism and geometry, particularly the area of its opening [12].

The pressure drop across the valve is

$$P_3 - P_4 = \rho K_v(t)V^2 \tag{6}$$

Substituting P_3, we have

$$\begin{aligned} P_4 &= P_{atm} - \rho K_f(t)V^2 - \rho L\frac{dV}{dt} - \frac{32\mu LV}{D^2} - \rho K_v(t)V^2 \\ \Rightarrow P_4 &= P_{atm} - \rho(K_f(t) + K_v(t))V^2 - \rho L\frac{dV}{dt} - \frac{32\mu LV}{D^2} \end{aligned} \tag{7}$$

As one would expect, the two loss coefficients K_f and K_v add up to form a combined loss coefficient that is representative of the losses across both the filter and the valve. These are the two time-varying "minor losses" in the system.

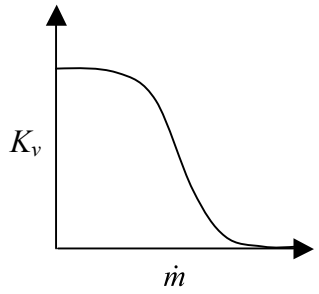

Figure 5 – A typical relationship between the loss coefficient K_v and mass flowrate $\dot{m}$ through a valve.

A typical curve relating K_v to $\dot{m}(t)$ is shown in Figure 5. The figure shows a dead-zone, a saturation effect, and an approximately linear section where operation typically takes place. The loss coefficient K_v is indirectly proportional to the control voltage of the valve. According to the manufacturer's datasheet, the valve has a loss coefficient of about 83 when it is fully open.

3.1.4 Vacuum Pump

Contrary to the other components in the system, the vacuum pump is expected to create a large pressure drop, which is necessary for performance. Referring to Figure 6, the pressure drop created by a vacuum pump is

$$\begin{aligned} P_5 - P_4 &= \Delta P_{\max} - K_p \dot{m} \\ \Rightarrow P_5 &= P_4 + \Delta P_{\max} - K_p \dot{m} \end{aligned} \tag{8}$$

where $\Delta P_{\max}$ is the maximum pressure drop that the pump can create, and K_p is a constant that characterizes the pump's performance as the rate required varies. Ideally, $K_p = 0$ means that the pump suffers no pressure loss regardless of the requested flowrate.

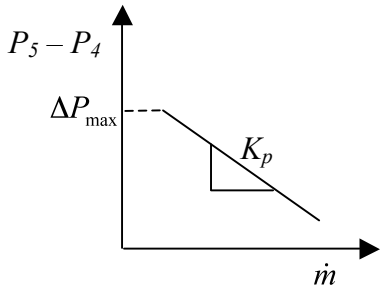

Figure 6 – Pump pressure-drop data typically provided by the manufacturer.

According to the manufacturer, the Robinair 15434 vacuum pump is rated at 20 microns Hg or 2.67 Pa, which is quite close to perfect vacuum, and has a free air displacement of 4 CFM or 113 LPM.

At zero flow, there will be a pressure drop

$$\Delta P_{\max} = P_5 - P_4\big|_{zerof\ low} = 1.013\times10^5 - 2.67 \approx 101.3\,kPa$$

At free air displacement, or zero pressure drop, the flow is 113 LPM, which is equivalent to 2.43×10^{-3} kg/s of air. From this information, we can calculate the slope of pump's characteristic curve:

$$Kp = 1.013\times10^5 \div 2.43\times10^{-3} = 4.17\times10^7\ Pa/(kg/s)$$

3.2 State-Space Model

We are now ready to compile the above information into one equation that expresses the dynamics of the system as a function of the mass flowrate. Looking back at the expression obtained for P_4 in (7), we will make the following substitution

$$\dot{m} = \rho V A \qquad \Rightarrow \quad V = \frac{\dot{m}}{\rho A}$$

Then,

$$P_4 = P_{atm} - (K_f(t) + K_v(t))\frac{\dot{m}^2(t)}{\rho A^2} - \frac{L}{A}\ddot{m}(t) - \frac{32\mu L}{\rho D^2 A}\dot{m}(t)$$

Finally, let $P_5 = P_{atm}$, substitute these into the expression for P_5 in (8), and reverse the signs

$$0 = \frac{L}{A}\ddot{m}(t) + \left(\frac{32\mu L}{\rho D^2 A} + K_p\right)\dot{m}(t) + (K_f(t) + K_v(t))\frac{\dot{m}^2(t)}{\rho A^2} - \Delta P_{\max} \tag{9}$$

This nonlinear equation relates the mass flowrate to the control input, $K_v(t)$, and the time-varying loss coefficient.

To write a state-space representation of this system, let $x_1 = m(t)$, $x_2 = \dot{m}(t)$ and $u = K_v(t)$ so that the system becomes

$$\dot{x}_1 = x_2$$

$$\dot{x}_2 = -\frac{K_f(t)}{\rho A L}x_2^2 - \left(\frac{K_p A}{L} + \frac{32\mu}{D^2}\right)x_2 + \frac{A}{L}\Delta P_{\max} - \frac{x_2^2}{\rho A L}u$$

3.3 Feedback Linearization and Trajectory Tracking

The objective is for the mass flowrate x_2 to track a certain desired trajectory $y_R(t)$, or in other words for the error $e = x_2 - y_R(t)$ to go to zero. We will design a feedback linearizing controller to accomplish this task.

Consider a nonlinear system of the form

$$\dot{x} = f(x) + g(x)u$$
$$y = h(x)$$

It is possible to transform this system into an equivalent linear system via the following state feedback control

$$u = \alpha(x) + \beta(x)v$$

where

$$\alpha(x) = -\frac{L_f{}^{\rho} h(x)}{L_g L_f{}^{\rho-1} h(x)}$$

$$\beta(x) = \frac{1}{\gamma(x)} = \frac{1}{L_g L_f{}^{\rho-1} h(x)}$$

L_f and L_g are the lie derivatives, and ρ is the relative degree of the system [6]. The relative degree of our system is one, and so we have

$$L_f h(x) = \frac{\partial h}{\partial x} f(x)$$
$$L_g L_f h(x) = \frac{\partial}{\partial g} L_f h(x)$$

With this form of control input, the overall system becomes linear and may be stabilized with a state-feedback controller $v = -Kx$.

To achieve trajectory tracking, the control law is modified as such

$$u = \alpha(x) + \beta(x)[v + y_R^{(\rho)}(t)]$$

which for our system becomes

$$u = \alpha(x) + \beta(x)[v + \dot{y}_R(t)]$$

The state-space model of the smoking machine is rewritten here

$$\begin{aligned} \dot{x}_1 &= x_2 \\ \dot{x}_2 &= -\frac{K_f(t)}{\rho AL} x_2^{\,2} - \left(\frac{K_p A}{L} + \frac{32\mu}{D^2} \right) x_2 + \frac{A}{L} \Delta P_{\max} - \frac{x_2^{\,2}}{\rho AL} u(t) \\ y &= x_2 \end{aligned} \tag{10}$$

For convenience, let

$$\begin{aligned} & f_1(x) = x_2, \quad g_1(x) = 0 \\ & f_2(x) = -\frac{K_f(t)}{\rho AL} x_2^{\,2} - \left(\frac{K_p A}{L} + \frac{32\mu}{D^2} \right) x_2 + \frac{A}{L} \Delta P_{\max}, \quad g_2(x) = -\frac{x_2^{\,2}}{\rho AL} \\ & h(x) = y = x_2 \end{aligned}$$

For a relative degree of one, the lie derivatives are computed as follows

$$\begin{aligned} L_f h(x) &= \frac{\partial h}{\partial x_1} f_1 + \frac{\partial h}{\partial x_2} f_2 \\ &= f_2 \\ &= -\frac{K_f(t)}{\rho AL} x_2^{\,2} - \left(\frac{K_p A}{L} + \frac{32\mu}{D^2} \right) x_2 + \frac{A}{L} \Delta P_{\max} \end{aligned}$$

and,

$$L_g L_f{}^0 h(x) = L_g h(x) = \frac{\partial h}{\partial x} g(x) = \frac{\partial h}{\partial x_1} g_1 + \frac{\partial h}{\partial x_2} g_2$$
$$= g_2$$
$$= -\frac{x_2{}^2}{\rho A L}$$

Therefore,

$$\alpha(x) = -\frac{f_2}{g_2}$$
$$\beta(x) = \frac{1}{g_2}$$

The overall feedback linearizing and tracking control law is

$$u = -\frac{f_2}{g_2} + \frac{1}{g_2}\left[v + \dot{y}_R(t)\right]$$
$$= \frac{1}{g_2}\left[-f_2 + v + \dot{y}_R(t)\right]$$
$$\Rightarrow u = -\frac{\rho A L}{x_2{}^2}\left[\frac{K_f(t)}{\rho A L} x_2{}^2 + \left(\frac{K_p A}{L} + \frac{32\mu}{D^2}\right) x_2 - \frac{A}{L}\Delta P_{\max} + v + \dot{y}_R(t)\right]$$

Clearly, the control input will be unbounded if x_2 is ever zero. With a small perturbation, this problem can be avoided. Let,

$$u = -\frac{\rho A L}{x_2{}^2 + \varepsilon}\left[\frac{K_f(t)}{\rho A L} x_2{}^2 + \left(\frac{K_p A}{L} + \frac{32\mu}{D^2}\right) x_2 - \frac{A}{L}\Delta P_{\max} + v + \dot{y}_R(t)\right] \qquad (11)$$

In tracking control, it is often useful to look at the error dynamics. We have previously defined the error as $e = x_2 - y_R(t)$. Then the derivative is

$$\dot{e} = \dot{x}_2 - \dot{y}_R(t)$$
$$= -\frac{K_f(t)}{\rho A L} x_2{}^2 - \left(\frac{K_p A}{L} + \frac{32\mu}{D^2}\right) x_2 + \frac{A}{L}\Delta P_{\max} - \frac{x_2{}^2}{\rho A L} u(t) - \dot{y}_R(t)$$

Substituting the linearizing tracking control law and carrying out all the appropriate cancellations, what remains is simply $\dot{e} = v$. To regulate the error, we choose an input of the form $v = -Ke$, where $K > 0$. In terms of the original states, the closed loop system now looks like this:

$$\begin{aligned} \dot{x}_1 &= x_2 \\ \dot{x}_2 &= v + \dot{y}_R(t) = -Ke + \dot{y}_R(t) \end{aligned}$$

To diminish the effect of a steady-state error, we will augment the system with an integral action over the error: $v = -K_1 e - K_2 \int e$.

Now the closed-loop system has the following form

$$\begin{aligned} \dot{x}_1 &= \dot{x}_2 \\ \dot{x}_2 &= -K_1 e - K_2 \int e + \dot{y}_R(t) \end{aligned} \tag{12}$$

The gains, K_1 and K_2, must both be positive, but the integral gain will likely be significantly smaller than the proportional gain. These gains can be tuned rather easily through simulation or experimentation.

3.4 Conclusion

Using fluid dynamics first principles, this chapter has expressed the dynamics of the smoking machine in a nonlinear state-space form, for which a feedback linearizing trajectory tracking controller has been designed. With a more practical view, we design an adaptive lookup table in the next chapter.

Chapter 4

Flow Control using an Adaptive Lookup Table

In the previous chapter, we saw that the system is a nonlinear one with time-varying dynamics. In fact, simply by looking at the characteristics of the various components, one can see that the system response will exhibit nonlinearities such as a dead-zone and saturation. Another complication is the time-varying component due to particulate matter accumulating on the collection filters.

The second control strategy, which is developed in this chapter, considers the system as a black-box with only input and output data available. This flow control algorithm has been based on an adaptive lookup table. Lookup tables capture the input-output map of a system. They are especially useful when the system consists of a combination of mechanical, electrical and software components [7]. Because our system is time-varying, a static lookup table will not work and so it is designed to adapt to changing circumstances. Maintaining the lookup table throughout an experiment guarantees

continuous improvement of the data and the representation of system's dynamic behavior in real-time.

4.1 Generating the Initial Lookup Table

Prior to reproducing a recorded smoking session, a calibration of the entire experimental setup is performed to generate the initial lookup table. This is achieved by sending a series of incremental voltages of size Δv to the proportional valve, from the fully closed to the fully open position, and recording the respective flowrates from the flow sensor. A typical lookup table for this type of system, shown in Figure 7, has a dead zone, a somewhat linear portion, and a saturation level.

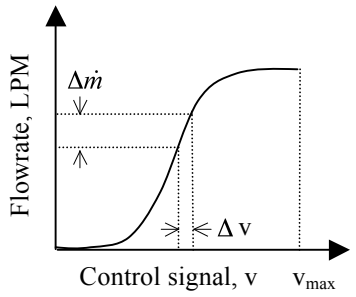

Figure 7 – Typical shape of a lookup table for the smoking machine. It relates the flowrate, measured by the flow sensor, to the required voltage, issued to the control valve.

Rather than making approximations on a large scale and reducing the accuracy of the controller, the table is regarded as piecewise linear in each $(\Delta v, \Delta\dot{m})$ interval, which can be made as small as needed.

4.2 Tracking a Smoking Session

The smoking machine loads a recorded smoking session consisting of a time series of flowrate data, which is the desired flow trajectory. The algorithm then reads the data point-by-point at the same frequency that it was recorded. At each sampling interval, the controller searches for the current desired flowrate in the lookup table, and issues the corresponding voltage to the proportional valve. If the exact flowrate is not found, the controller searches for its closest neighborhood and interpolates linearly within that interval.

4.3 The Learning Process

The dynamics of the smoking machine are continuously changing, mostly due to the clogging filters, but also due to other factors, such as particulates depositing on the sides of the pipes and tubing, and even the bubbling of the water in the narghile during a puff. Similarly, in a cigarette, one would expect the dynamics to change as it burns.

To ensure proper trajectory tracking as these changes take effect, the lookup table statistically learns from new data it receives throughout the experiment. As flow becomes more restricted in the system, it follows that the proportional valve should be opened further to achieve the same desired set point. Consequently, the lookup curve will shift to the right as shown in Figure 8.

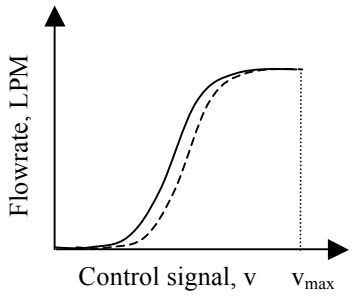

Figure 8 – The flow-voltage curve shifts to the right as flow becomes more restricted.

In practice, this is done on an entry-by-entry basis. Let $\dot{m}(k)$ and v*(k)* be entries in the current lookup table at time instant *k*. The real-time adaptation algorithm continuously receives new flow-voltage points, $(\mathrm{v}'(k), \dot{m}'(k))$. It begins by searching for an entry equal to $\dot{m}'(k)$, and if found, compares the corresponding voltage in the lookup table v*(k)* to the newly received v'*(k)*. If those are different, the old value is replaced with the new one. If, however, the exact entry for $\dot{m}'(k)$ is not found, the algorithm searches for the nearest neighbor to $\dot{m}'(k)$ and replaces the old value with the average of the old and new values. Figure 9 illustrates with an example.

Current lookup table	
Voltage	Flowrate
$v_1(k)$	$\dot{m}_1(k)$
$v_2(k)$	$\dot{m}_2(k)$
$v_3(k)$	$\dot{m}_3(k)$
$v_4(k)$	$\dot{m}_4(k)$
⋮	⋮

$\leftarrow \dot{m}'(k)$
Nearest neighbor to $\dot{m}'(k)$ is $\dot{m}_3(k)$

Updated lookup table	
Voltage	Flowrate
$v_1(k+1)$	$\dot{m}_1(k+1)$
$v_2(k+1)$	$\dot{m}_2(k+1)$
$v_3(k+1)$	$\dot{m}_3(k+1) = \frac{\dot{m}_3(k) + \dot{m}'(k)}{2}$
$v_4(k+1)$	$\dot{m}_4(k+1)$
⋮	⋮

Figure 9 – An example of how the lookup table learns from new information.

Following this procedure of averaging, an entry will have the following value n-iterations later

$$\underset{0 \le n \le N}{\dot{m}(k+n)} = \frac{\dot{m}(k)}{2^n} + \sum_{j=0}^{n-1} \frac{\dot{m}'(k+j)}{2^{n-j}} \tag{13}$$

Each new entry consists of a weighted average of previous entries, where more weight is placed on newer data. The table slowly forgets older values. Equation (13) can be rewritten as basically a discrete system that has the following dynamics

$$x(k+1) = \frac{1}{2}x(k) + \frac{1}{2}u \tag{14}$$

where $x(k) = \dot{m}(k)$ and $u = \dot{m}'(k)$.

Correcting the old entry with the average of the old and new data points serves a few purposes. First, the lookup table preserves some data history, which leads to improved learning. Second, the integrity of the lookup table is kept intact by not simply wiping out old entries with new ones that may be corrupt, such as measurement spikes.

Since the lookup table learns from new data it receives, only those flow-voltage points that are encountered in the experiment are corrected in the table. The system curve begins to look similar to Figure 10. Although learning is done on an entry-by-entry basis, the overall trend is for the points, and the curve as a whole, to shift to the right as flow resistance builds up in the system.

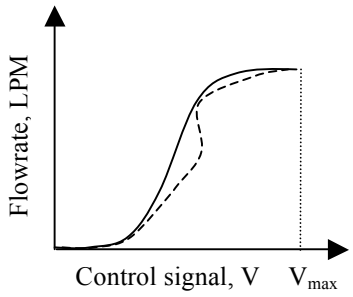

Figure 10 – Only those flow points encountered during an experiment are corrected in the lookup table.

One of the biggest advantages of using an adaptive lookup table approach is that no knowledge of the transfer function is needed. The system dynamics are built in to the lookup table when it is first generated and as it learns during an experiment. Therefore, changes to the experimental setup, such as a different smoking device or a different filter configuration, does not require knowledge of the new system dynamics. That is all taken into account at initial generation of the lookup table.

Moreover, system changes occurring during the experiment are quickly reflected by the lookup table. In essence, the lookup table is the system's dynamics, an input-output map that corrects itself progressively.

4.4 Conclusion

While in the previous chapter we made use of a mathematical description of the system dynamics, this chapter explored the design of an adaptive lookup table controller based

primarily on a practical understanding of the system. The following chapter compares these two approaches in terms of implementation complexity and performance.

Chapter 5

Comparison of the Controllers: Simulation and Experimentation

Now that we have laid down the design framework for the two controllers, we will illustrate the strengths and weaknesses of each approach through simulation and experimentation.

The time-varying parameter K_f is first assumed to be constant. For the type of filter used in [10], a typical K_f is 0.3 when it is still unused. As loading increases, so will K_f, until the filter is totally clogged and no longer allows any flow through it. This extreme case, however, does not happen in practice as each filter has a loading capacity, and is therefore replaced in the middle of an experiment between puffs. Consequently, the second variation of K_f is chosen to be a sawtooth signal.

As for reference inputs, three cases are considered; the classic step input, a periodic signal, and a recorded smoking pattern. For each case, we first keep K_f constant at 0.3 so that the dynamics of the system can be studied without the time-varying effects. The tests are then repeated given a sawtooth pattern for K_f.

We begin by studying the individual controllers, and proceed to a comparison of the two using the following performance measures: the error in total volume, average error in puff volume, and the convergence of the instantaneous error.

5.1 Feedback Linearizing Controller

5.1.1 Step Response

The step response of the system using the feedback loop controller is shown in Figure 11. The control signal $u = K_v(t)$ starts off very large and decreases to about 1900. Ideally, an infinite K_v means that the valve is absolutely closed and prohibits any flow. Practically, however, K_v can be clipped at some large number, here 10000, and still mean that flow is cut off. The gains of the PI controller were tuned to $K_1 = 25$ and $K_2 = 2$. Figure 13 shows how well the system responded to a sawtooth pattern in K_f. The control signal drops indicating a wider valve opening, as K_f ramps up.

The pressure drops across the four main components, shown in Figure 12 and Figure 14, illustrate some of the physical phenomena in the system. The pressure drop is analogous to a voltage drop in an electric circuit, as are the flow rate and filter flow coefficient to electric current and resistance, respectively. To maintain the desired flow rate of 12 LPM

as the pressure drop across the filter increases, the valve must act in an opposing direction. Consequently, as K_f increases, K_v must decrease. Initially, the pressure drop in the tube spikes due to the inertia of the slug of the fluid. The system exhibits a large pressure drop to overcome the fluid at rest.

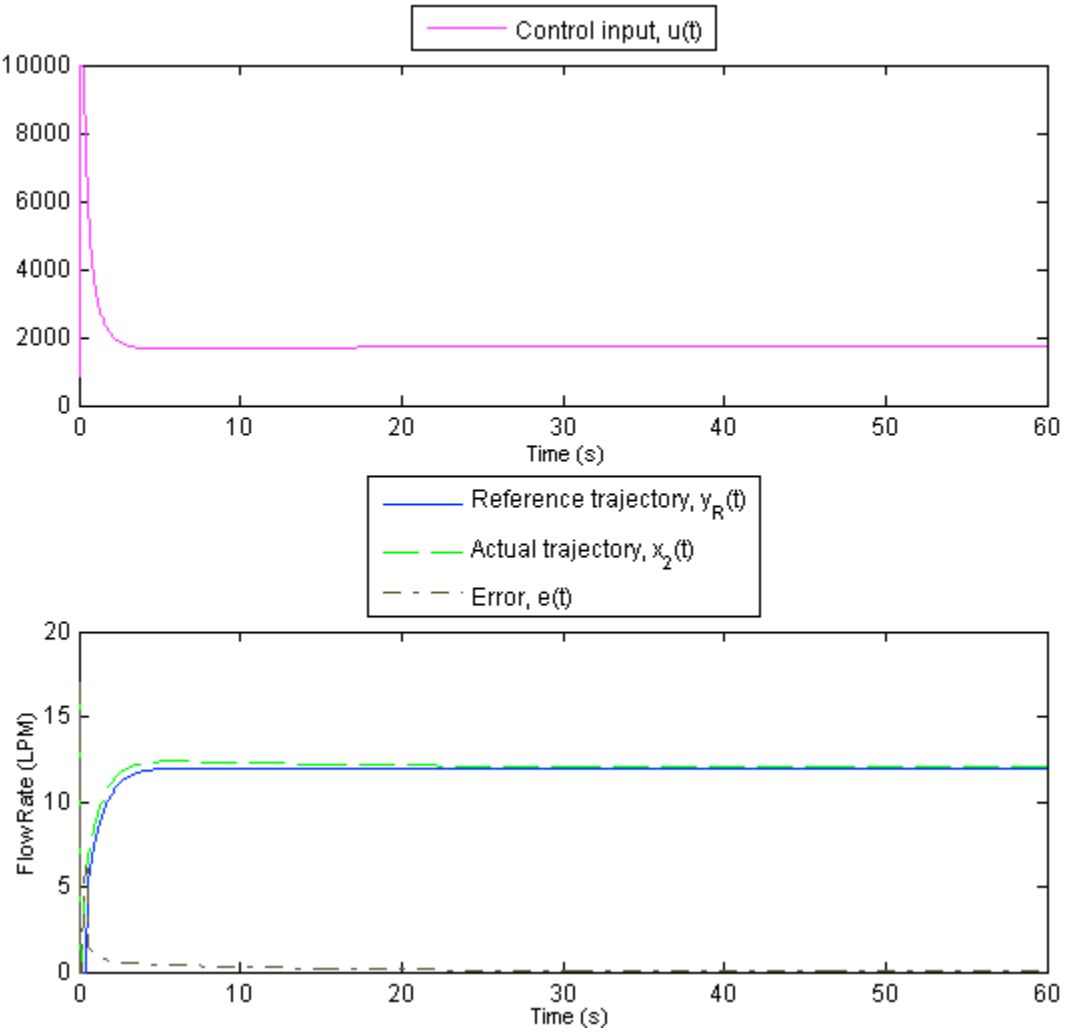

Figure 11 – Closed loop response using the feedback linearizing controller for a step input and constant K_f

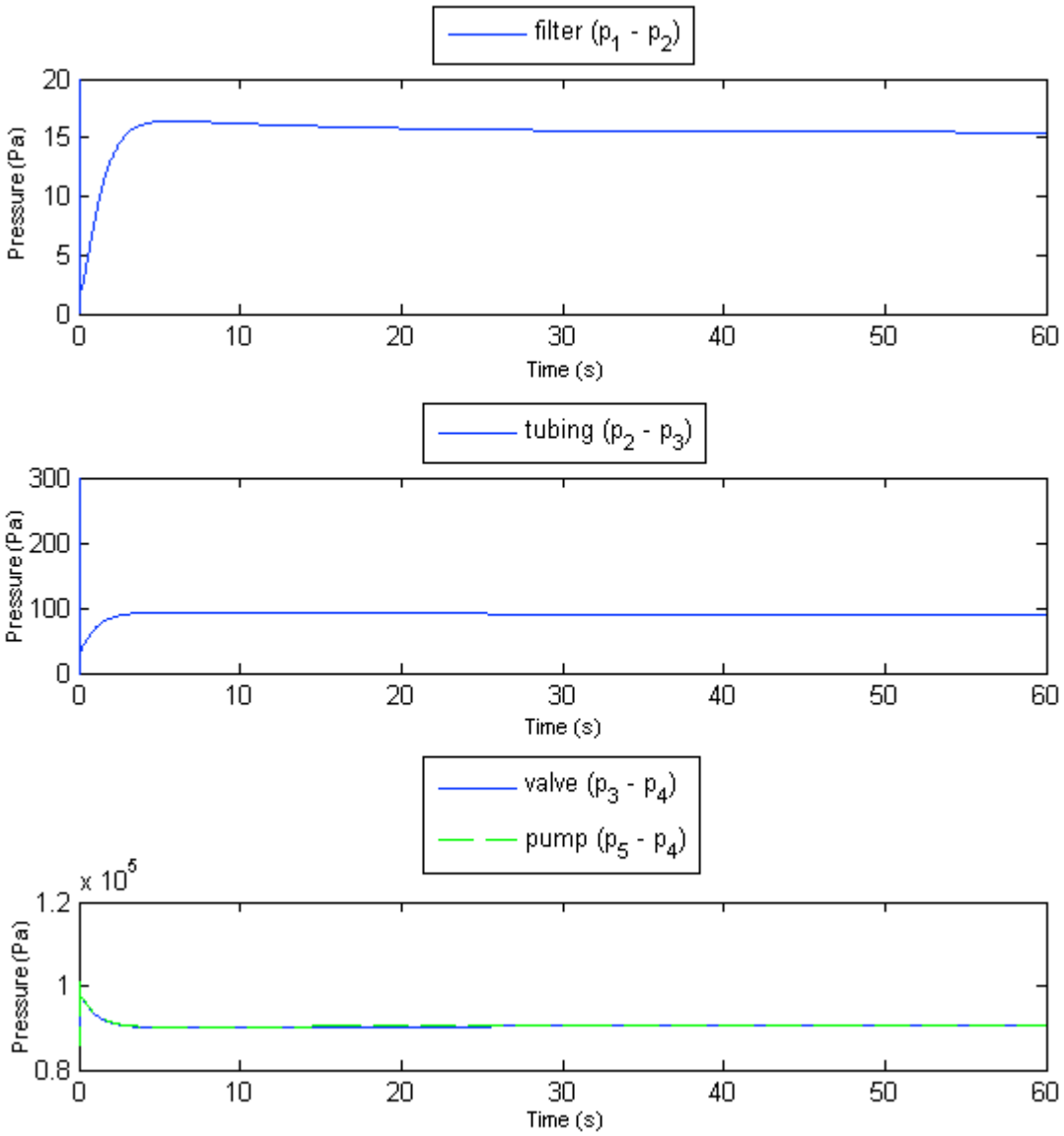

Figure 12 – Pressure drops in closed loop response using the feedback linearizing controller for a step input and constant K_f

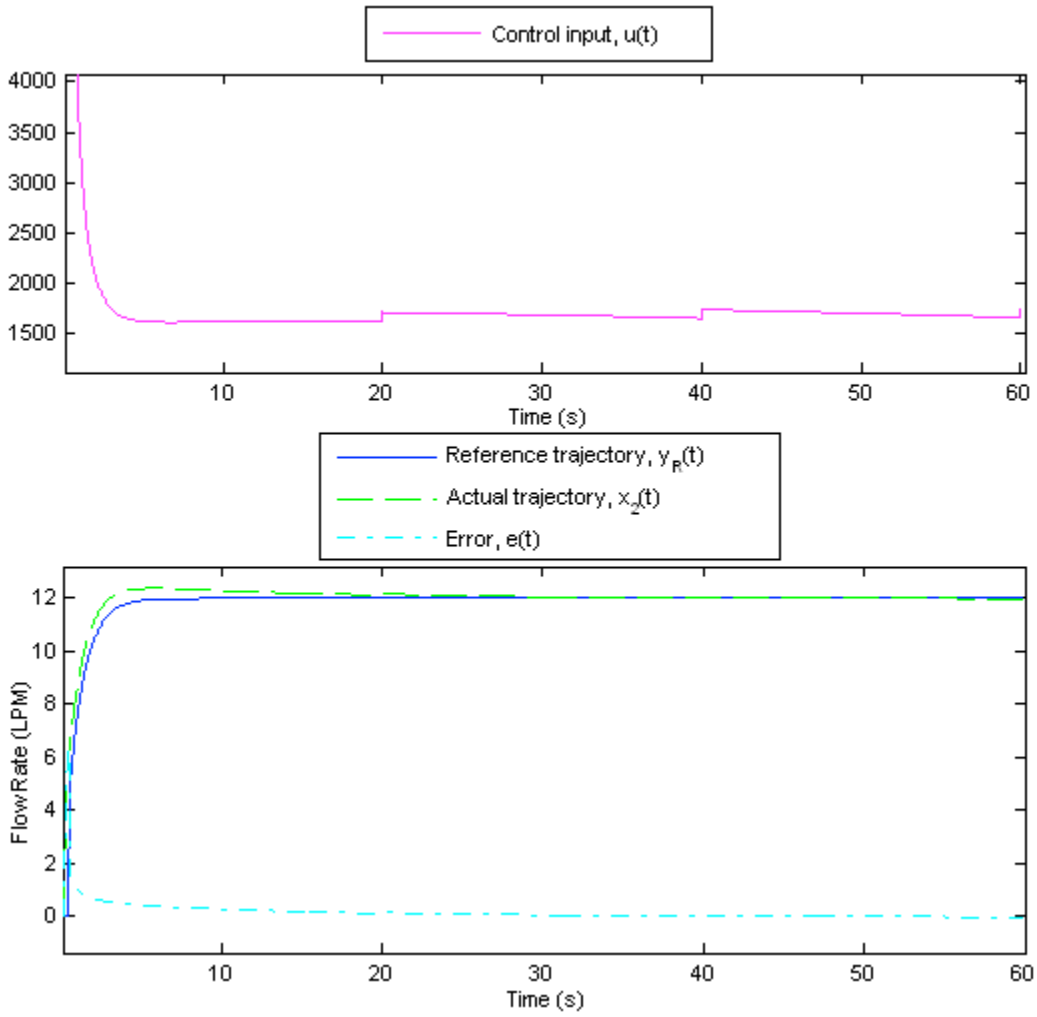

Figure 13 – Closed loop response using the feedback linearizing controller for a step input and sawtooth K_f

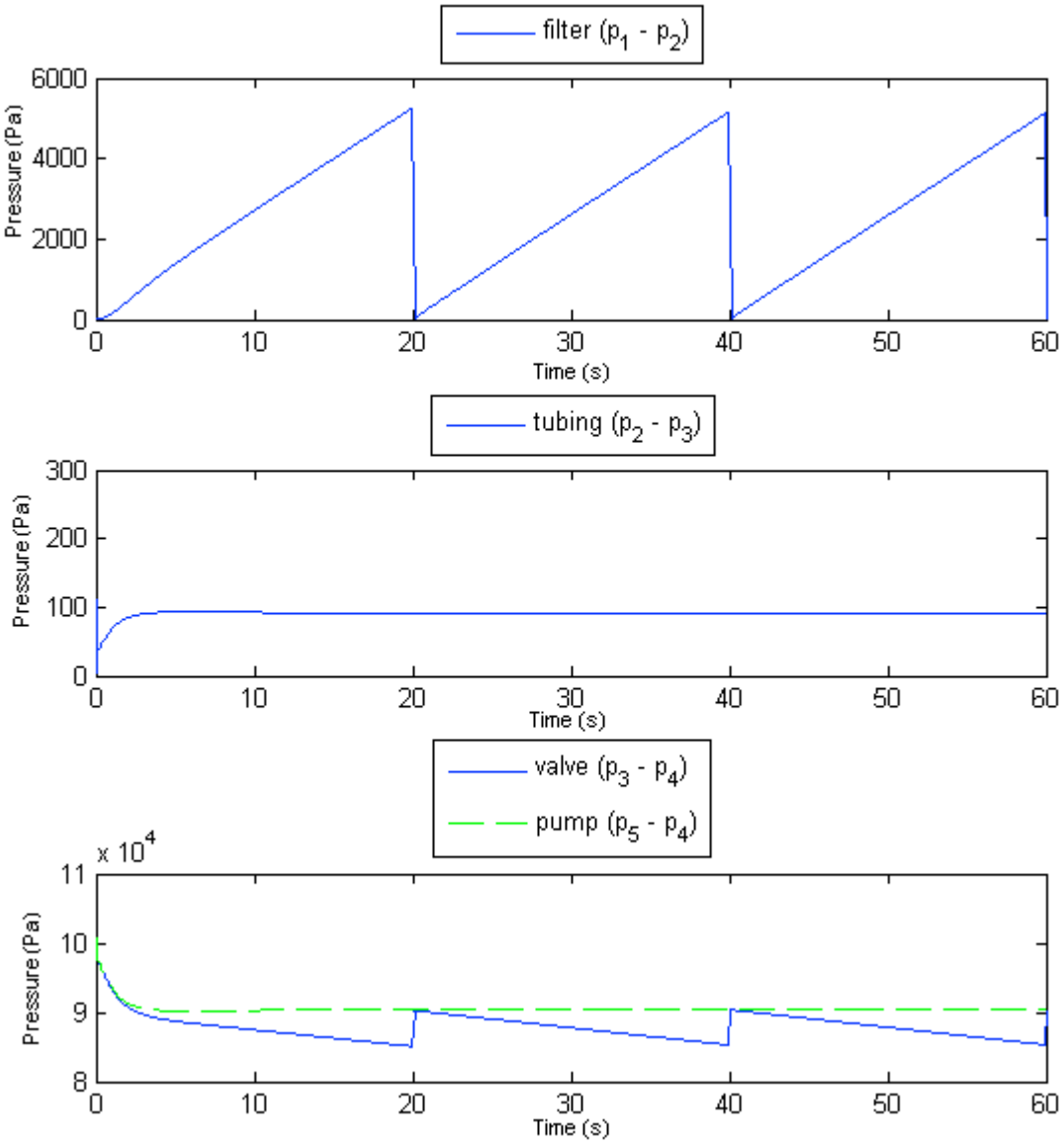

Figure 14 – Pressure drops in closed loop response using the feedback linearizing controller for a step input and sawtooth K_f

5.1.2 Periodic Reference

Current smoking machines generate periodic signals. The PI gains used for the step input were modified for this type of reference. Specifically, a smaller integral gain, 0.28, was used, since the gain of 2 used for the step response was too harsh in this case. It is known

that although an integral gain can eliminate steady-state error, it can make the transient response worse. So, for a periodic trajectory reference, a smaller integral action will slowly but surely diminish the steady-state error.

The responses and pressure drops are shown in Figures 15 through 18 respectively. An interesting spike effect is seen in the pressure drop across the tubing in Figures 16 and 18. At the beginning of a puff, the system overcomes friction and rushes to accelerate the fluid in the tubing, while at the end of a puff, the sudden closing of the valve causes a pressure build up.

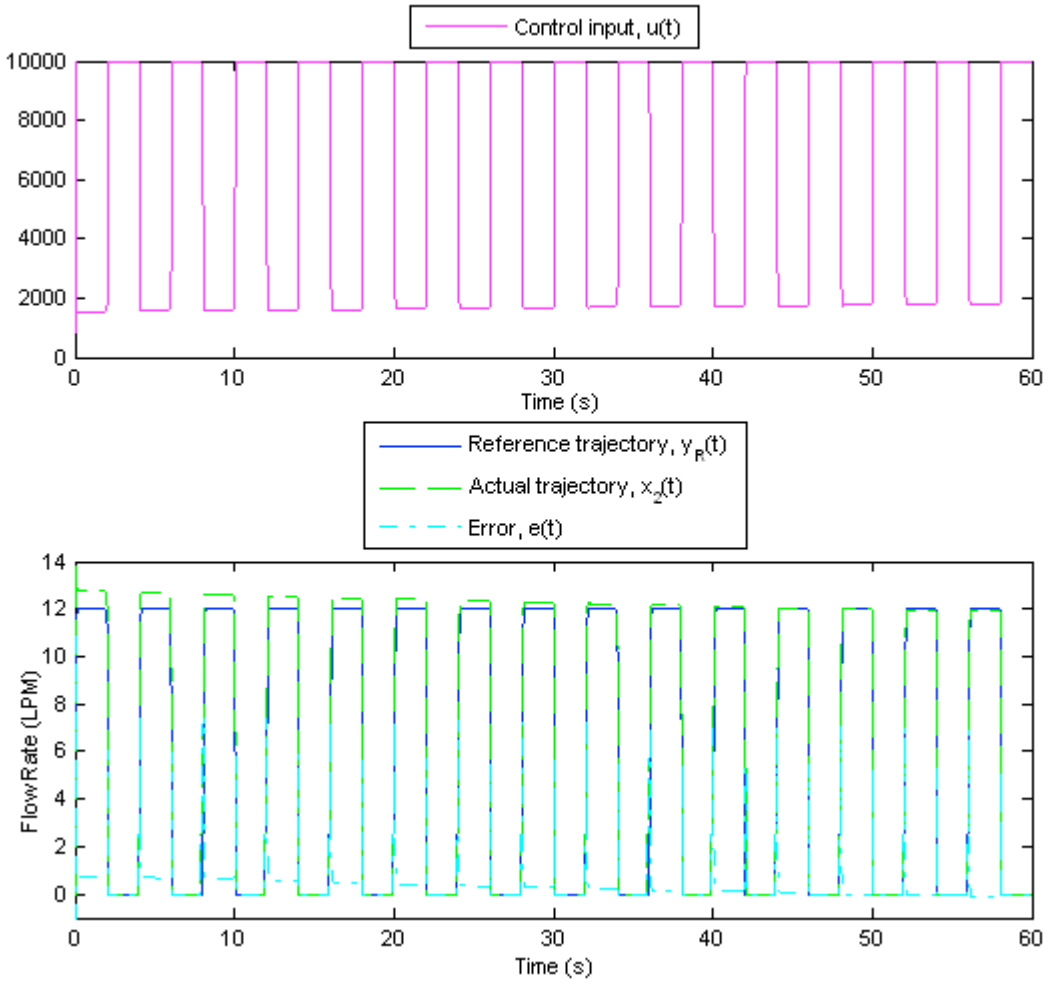

Figure 15 – Closed loop response using the feedback linearizing controller for a periodic input and constant K_f

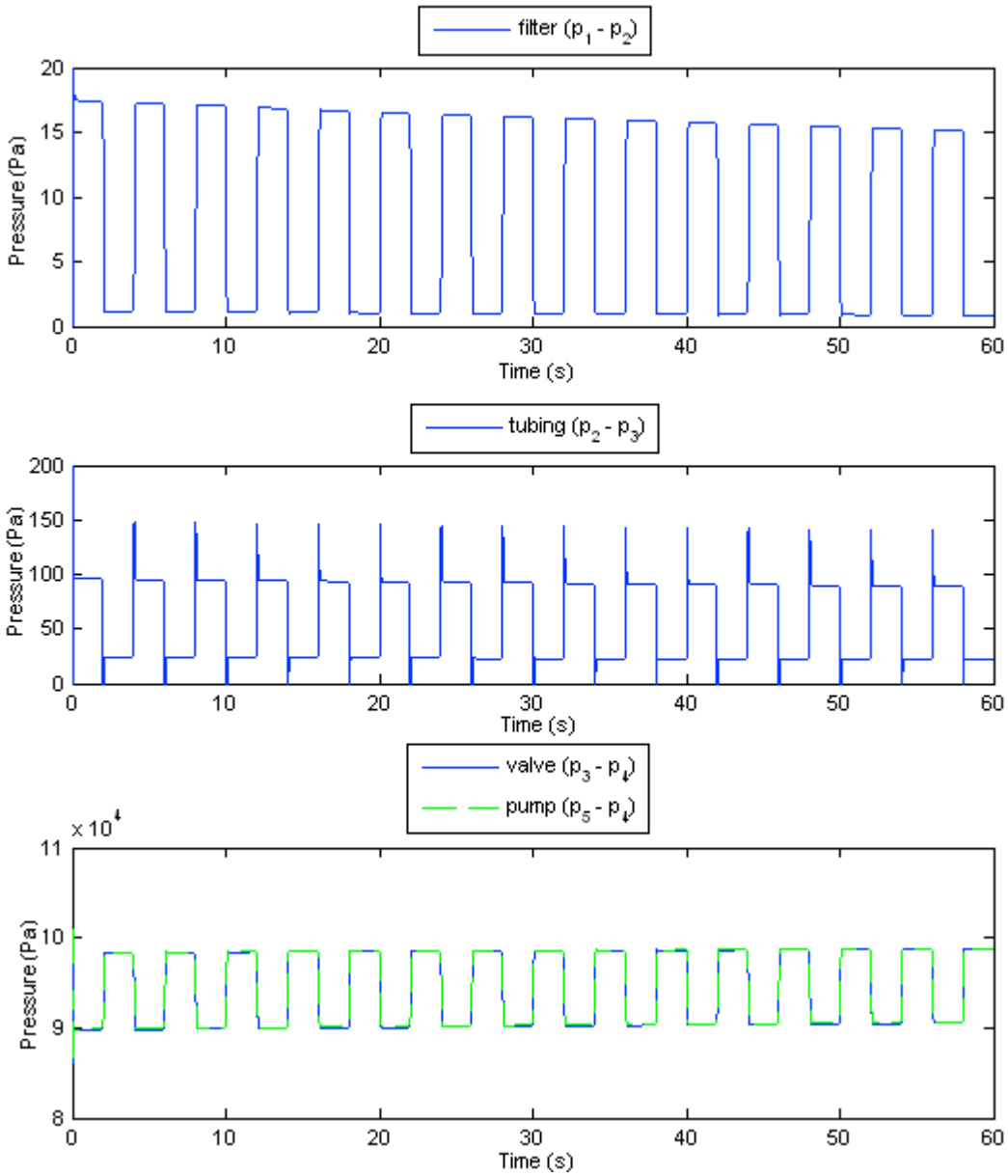

Figure 16 – Pressure drops in closed loop response using the feedback linearizing controller for a periodic input and constant K_f

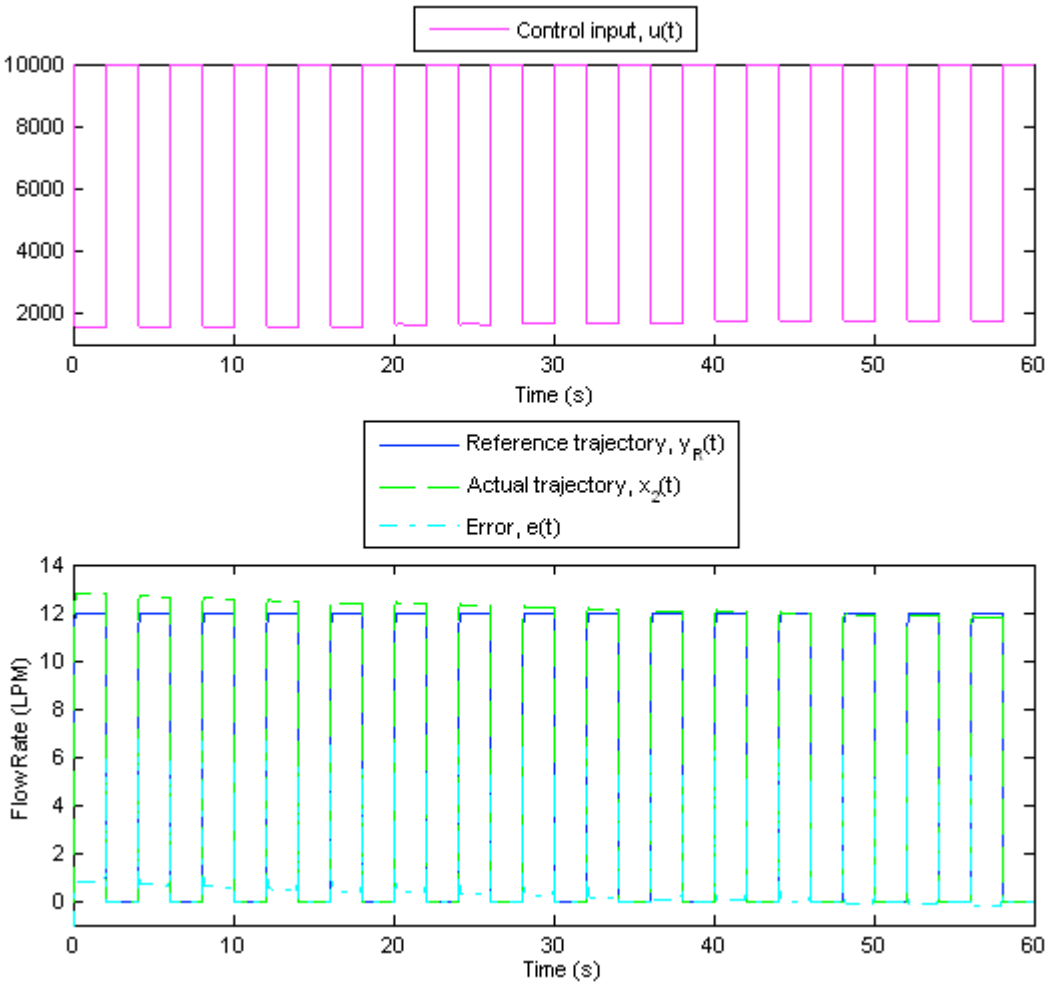

Figure 17 – Closed loop response using the feedback linearizing controller for a periodic input and sawtooth K_f

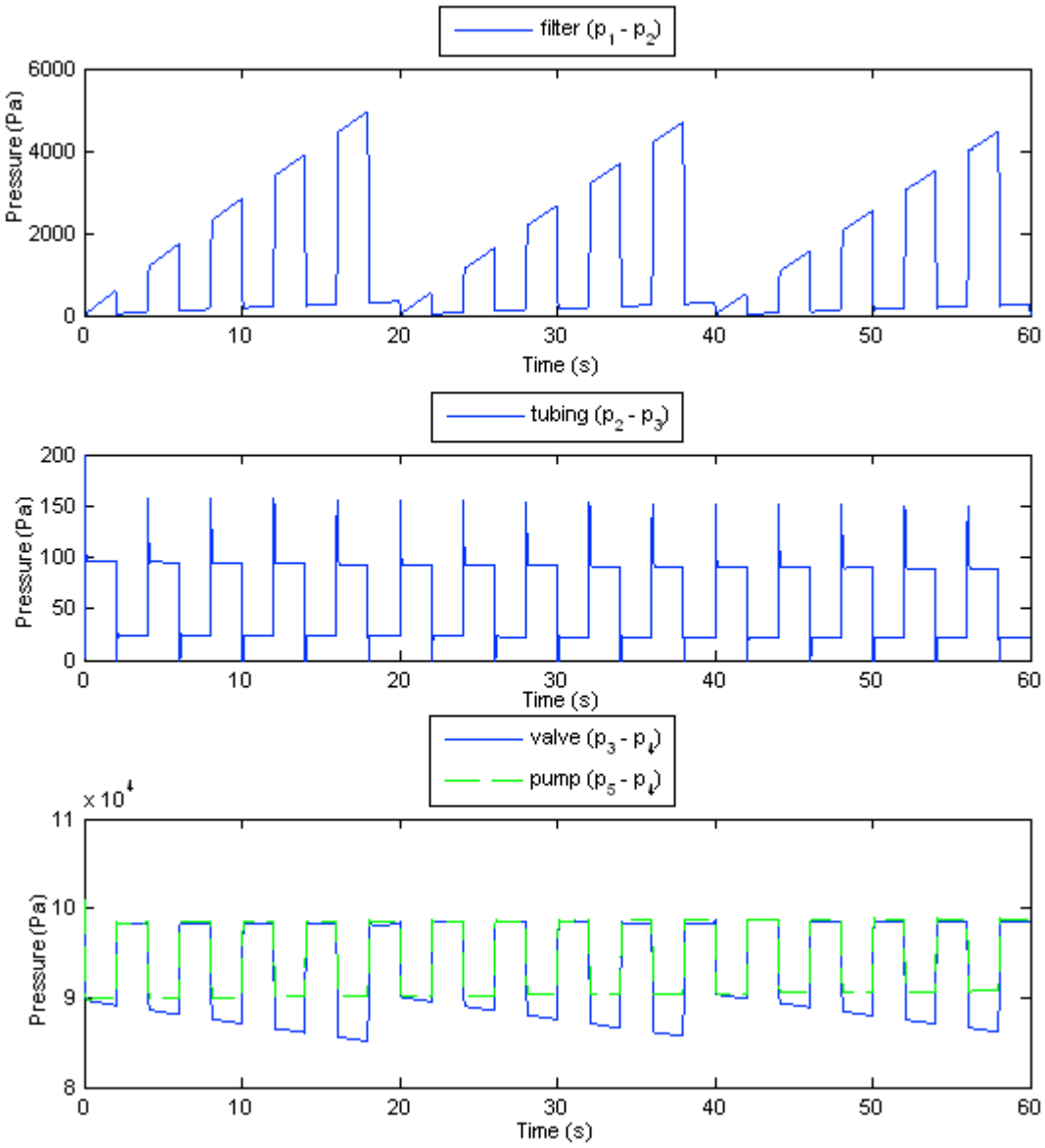

Figure 18 – Pressure drops in closed loop response using the feedback linearizing controller for a periodic input and sawtooth K_f

5.1.3 Recorded Reference

The most realistic reference trajectory for this application is, of course, recorded smoking patterns. Once again, the PI gains were further tuned to this reference. A large proportional gain of 50 was used and another relatively small integral gain of 0.5. The

higher proportional gain was needed to track the unpredictable smoking patterns, which have varying flow rates, puff and inter-puff durations. The overall response to this reference input is noteworthy, even with a sawtooth K_f. Figures 19 through 24 show the responses and pressure drops. A closer look at the response can be seen in Figures 20 and 23. These two puffs are examples of the lack of symmetry and predictability of smoking patterns in the narghile.

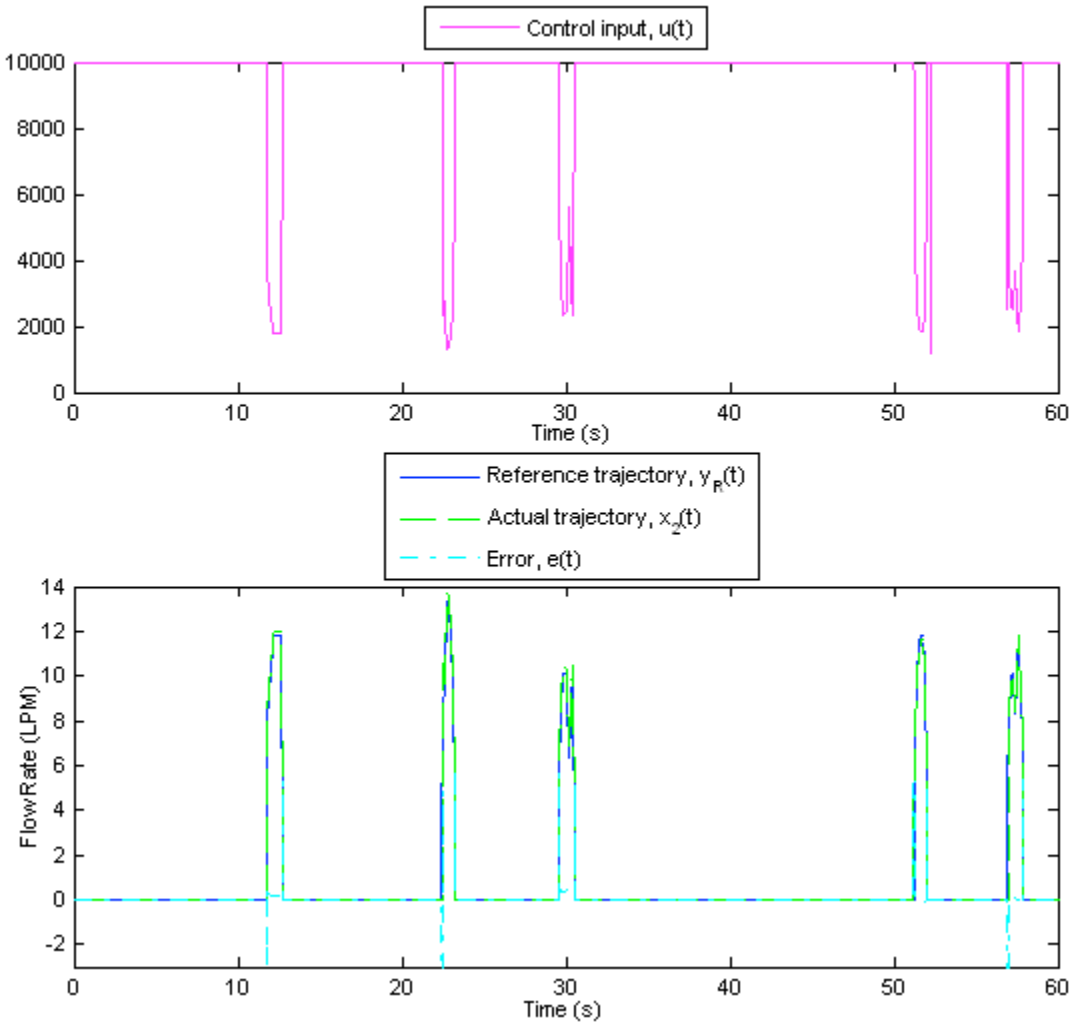

Figure 19 – Closed loop response using the feedback linearizing controller for a recorded input and constant K_f

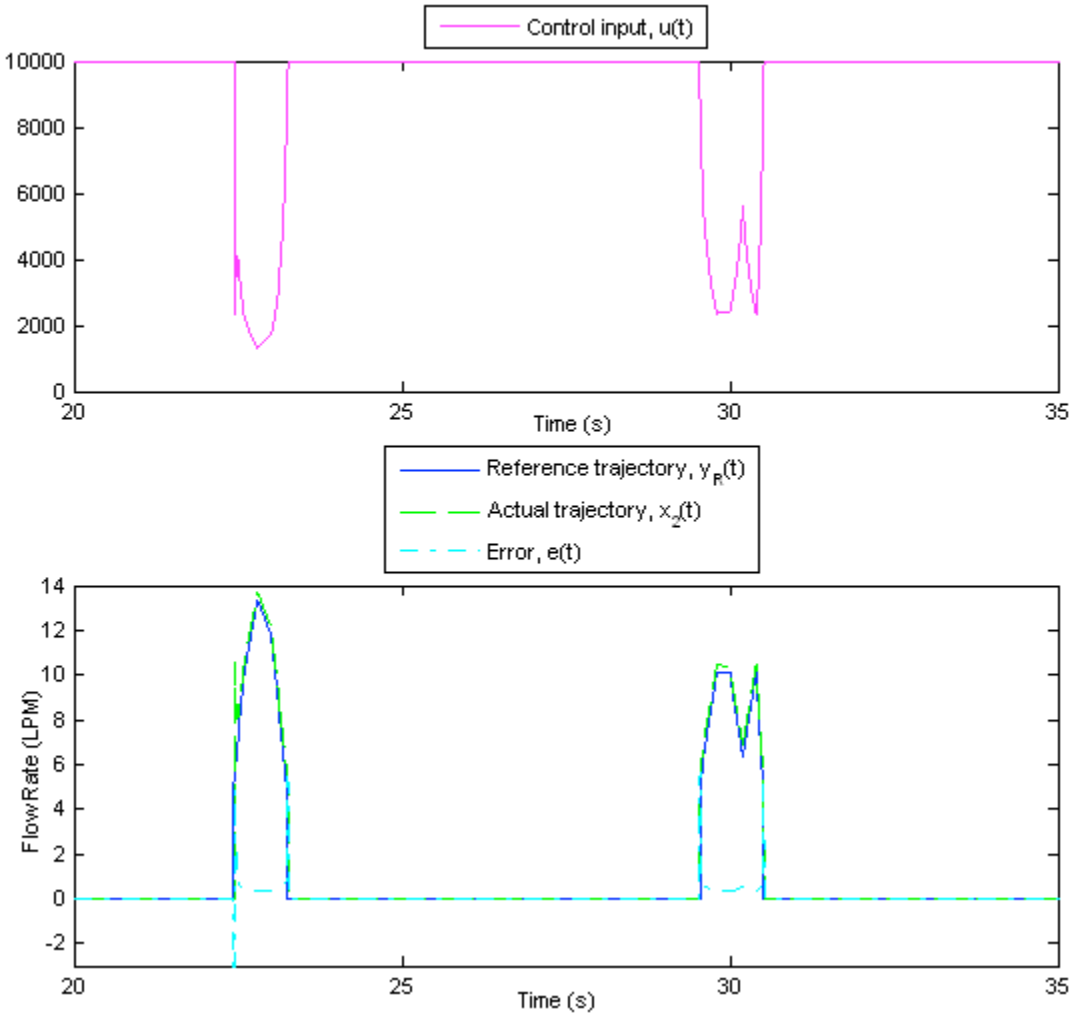

Figure 20 – Two-puff snapshot using the feedback linearizing controller for a recorded input and constant K_f

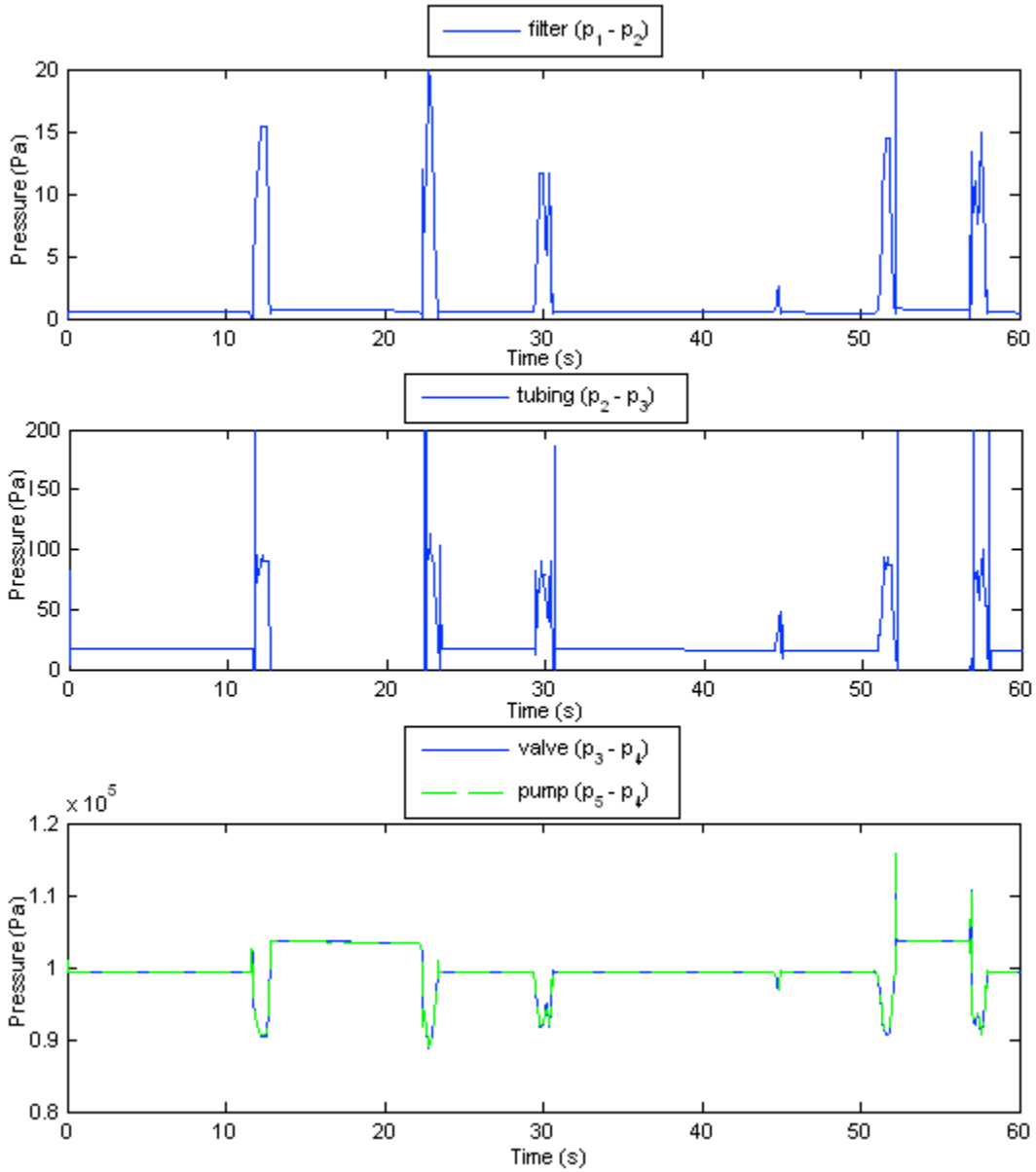

Figure 21 – Pressure drops in closed loop response using the feedback linearizing controller for a recorded input and constant K_f

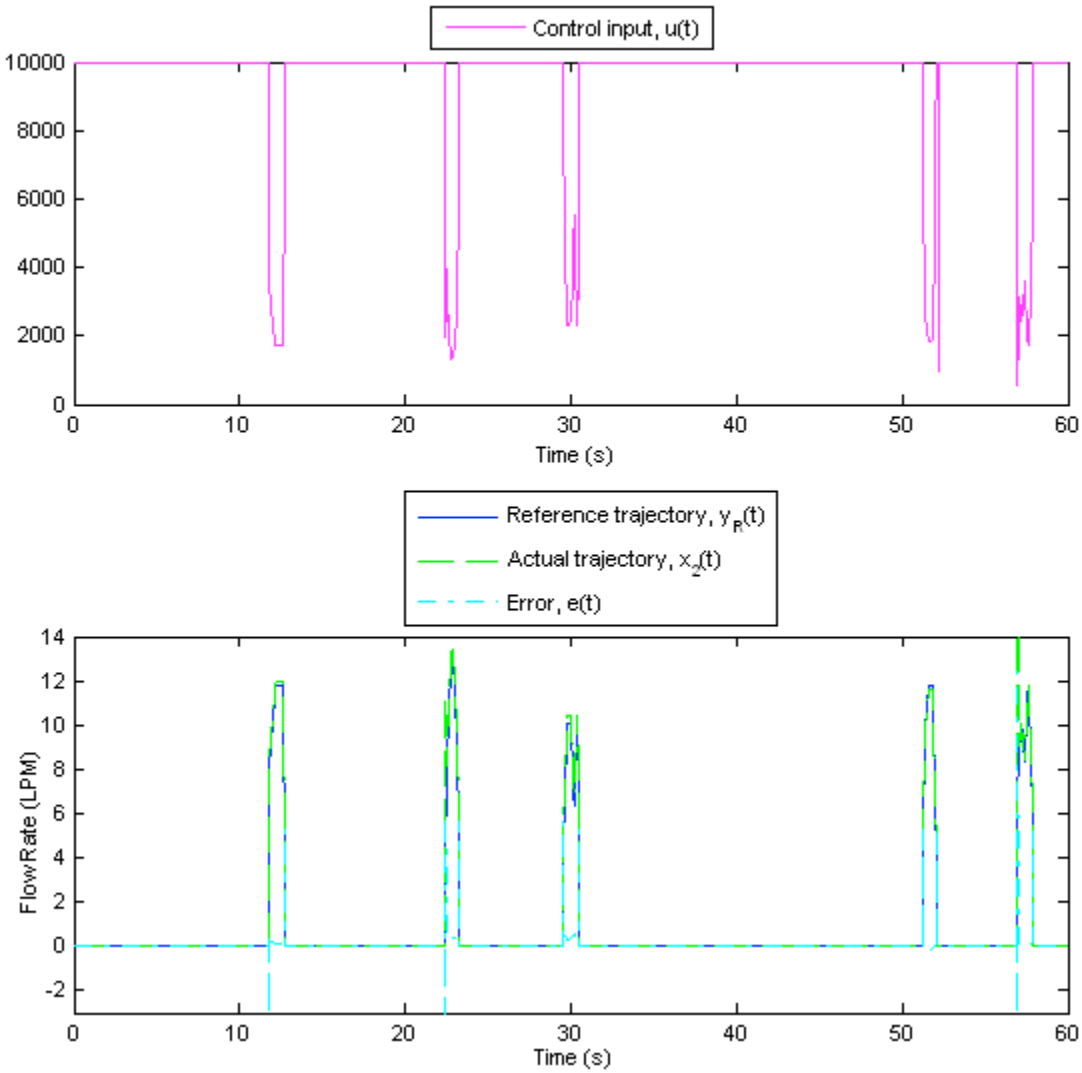

Figure 22 – Closed loop response using the feedback linearizing controller for a recorded input and sawtooth K_f

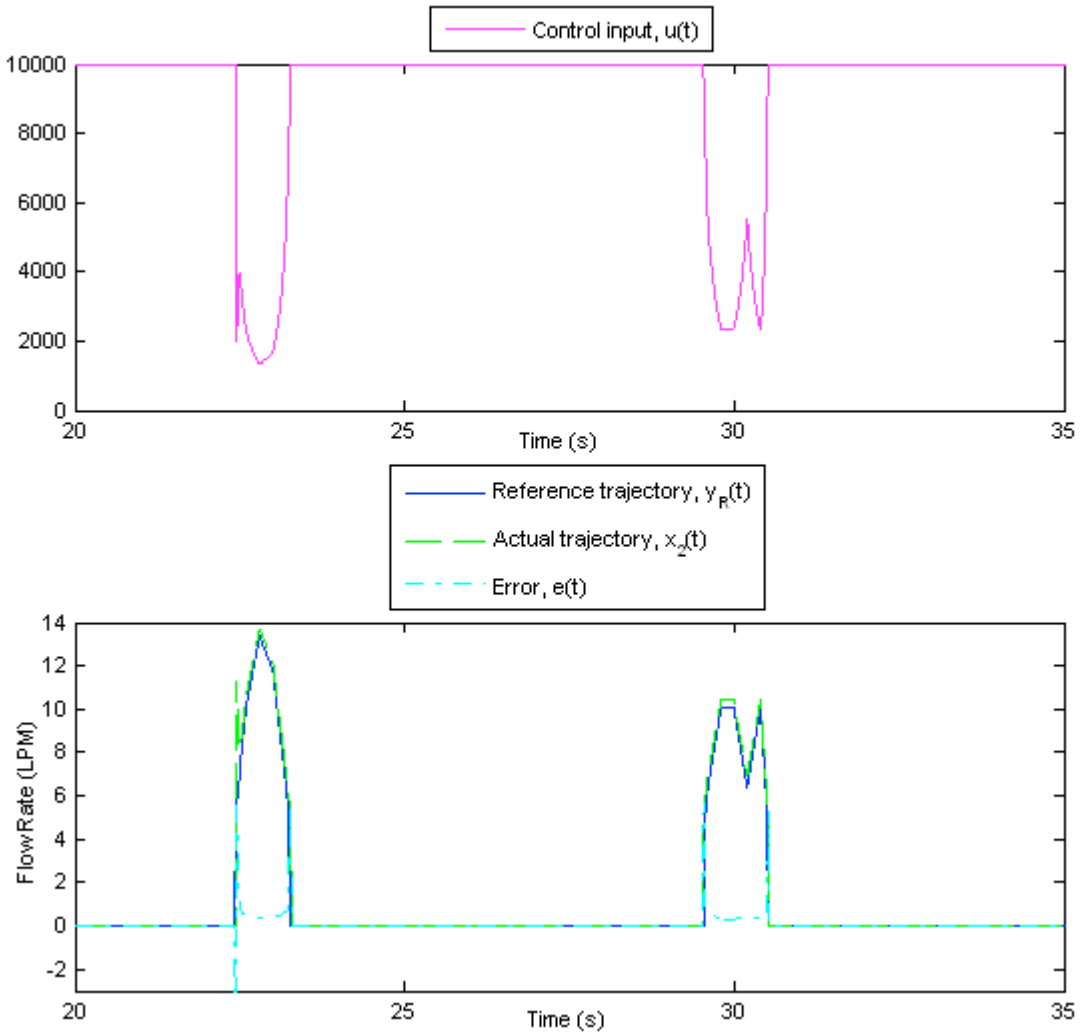

Figure 23 – Two-puff snapshot using the feedback linearizing controller for a recorded input and sawtooth K_f

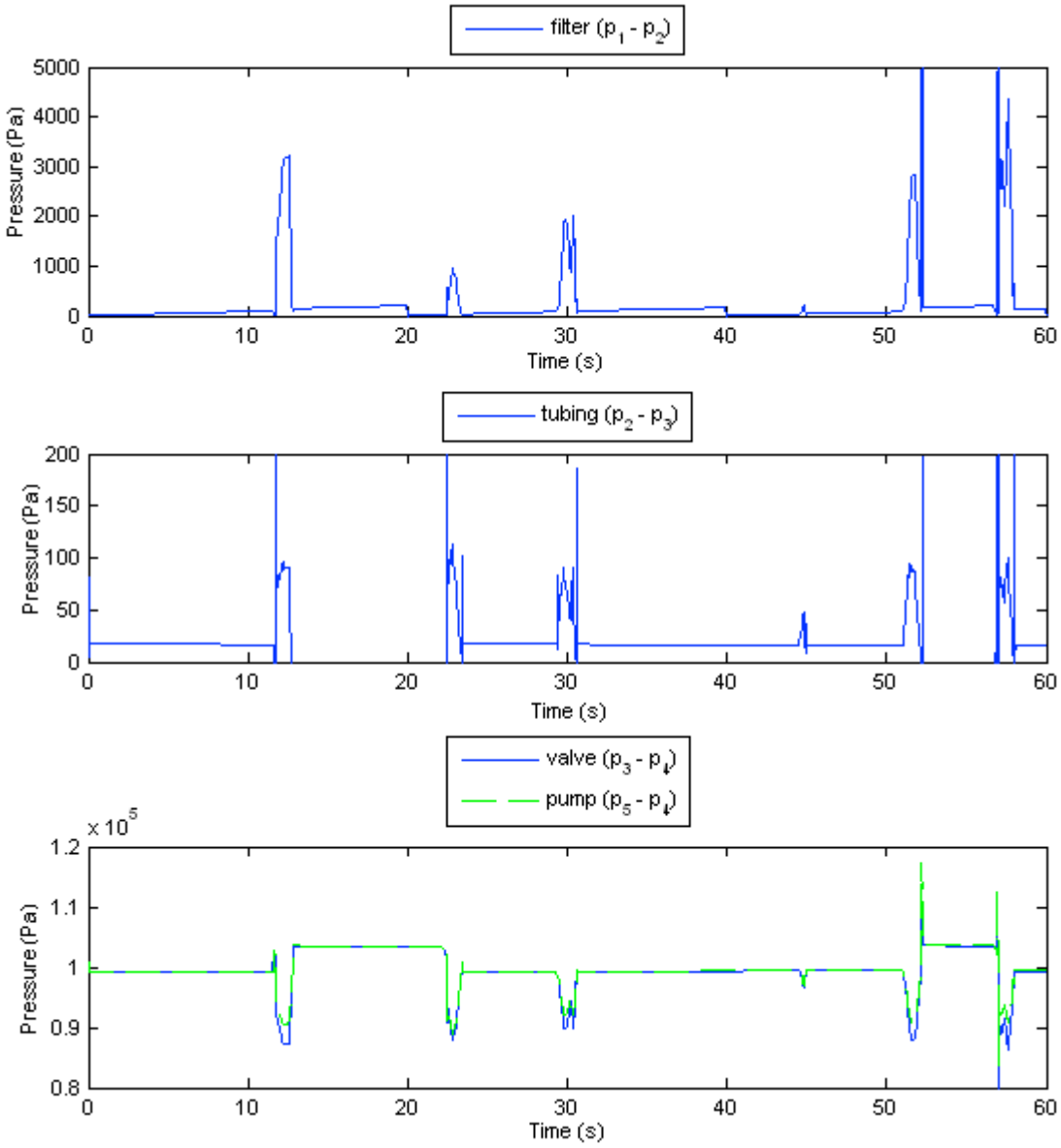

Figure 24 – Pressure drops in closed loop response using the feedback linearizing controller for a recorded input and sawtooth K_f

5.2 Adaptive Lookup Table

5.2.1 Step Response

The step response using the adaptive lookup table in Figure 25 shows significantly less error, despite minor oscillations around the set point. Since this response was generated from a physical implementation, the oscillations may be caused by measurement noise, but also by the iterative nature of the lookup table approach.

Pressure drop information from this setup is not available for lack of appropriate equipment, namely, pressure transducers. Nonetheless, the performance of this controller is quite remarkable as can be seen in the small errors even when a sawtooth filter flow coefficient is presented. See Figure 26. The filter flow coefficient was emulated by varying the opening of a second valve, which resulted in slightly higher control signals.

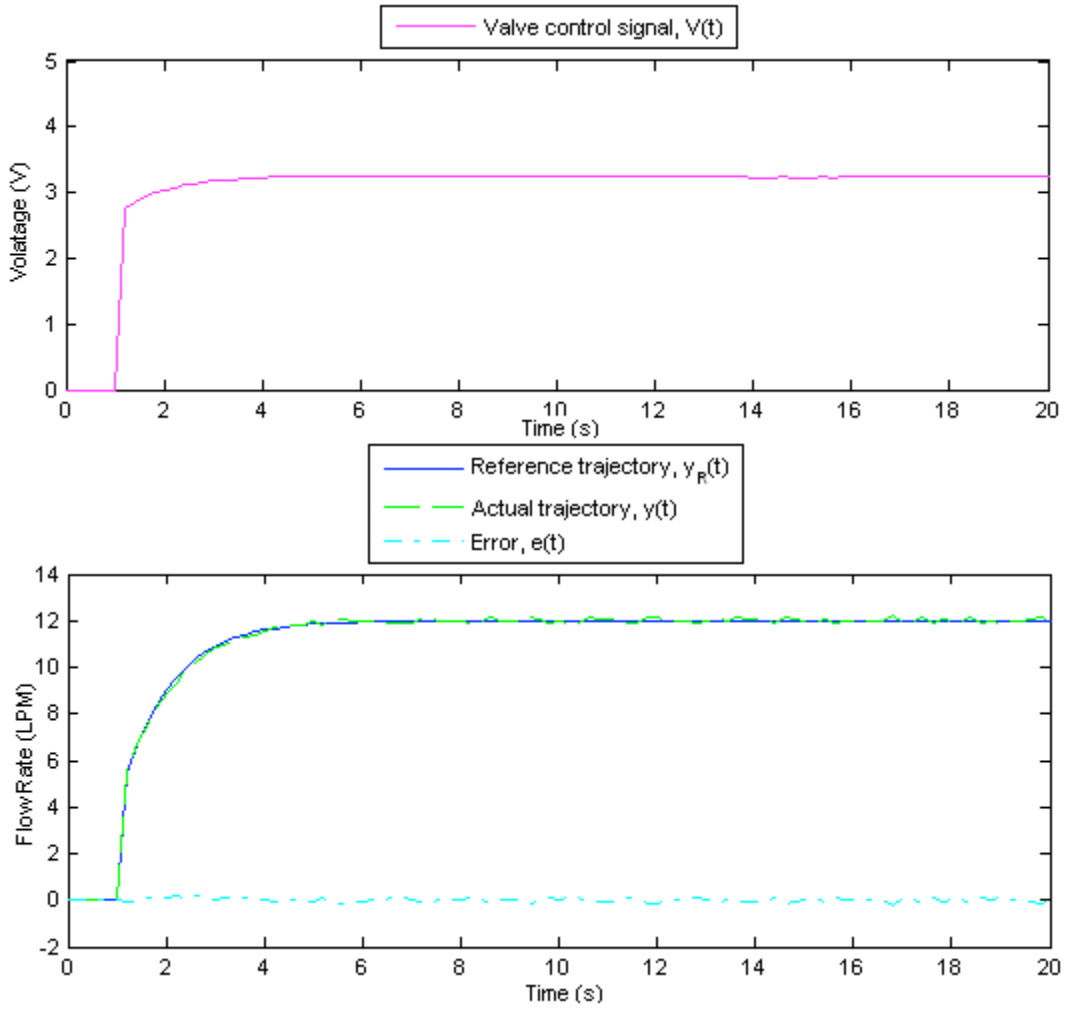

Figure 25 – System response using the adaptive lookup table approach for a step input and constant K_f

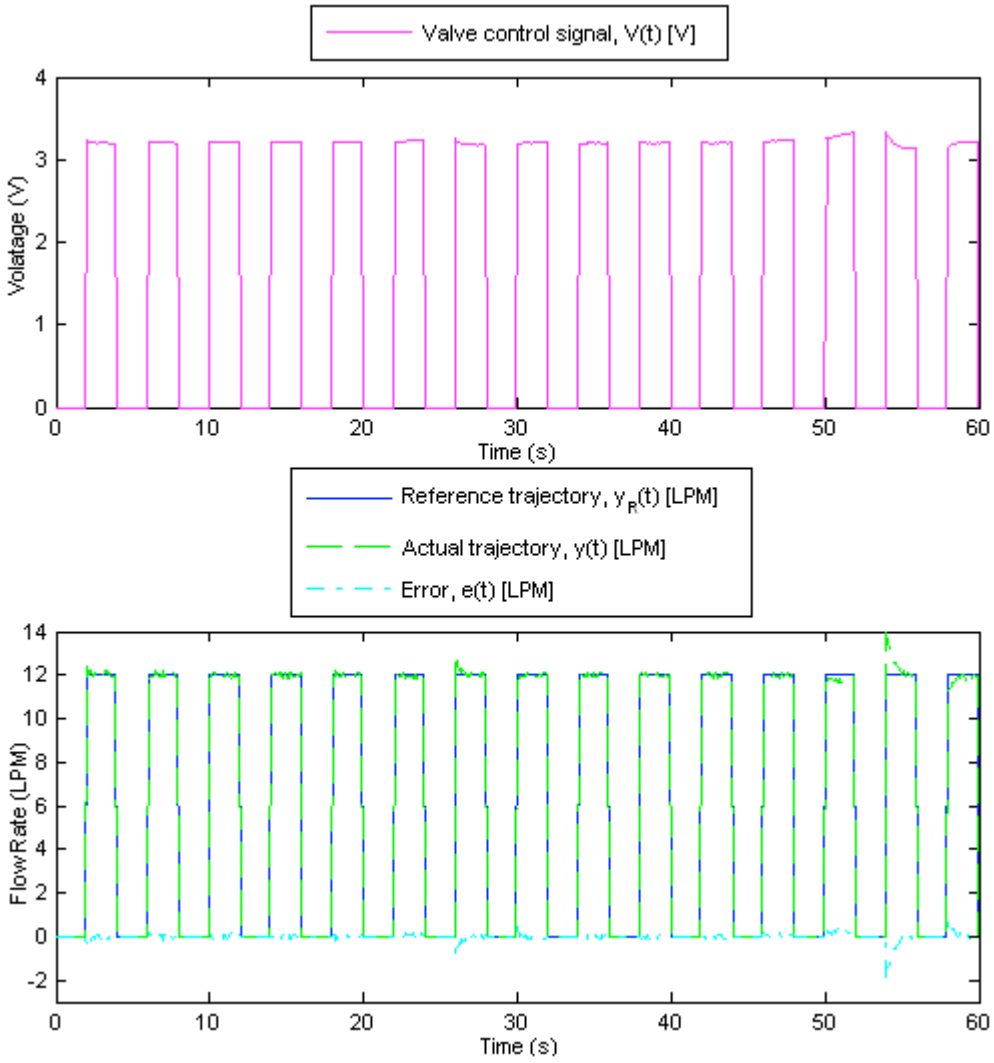

Figure 26 – System response using the adaptive lookup table approach for a step input and sawtooth K_f

5.2.2 Periodic Reference

Figures 27 and 28 illustrate the system response to a periodic input given a constant and sawtooth variation in flow resistance, respectively. In the case of the sawtooth pattern, a harsher resistance was given in the second to last puff, to see how quickly the response recovers. The oscillations during a puff are still visible, similar to those in the step response.

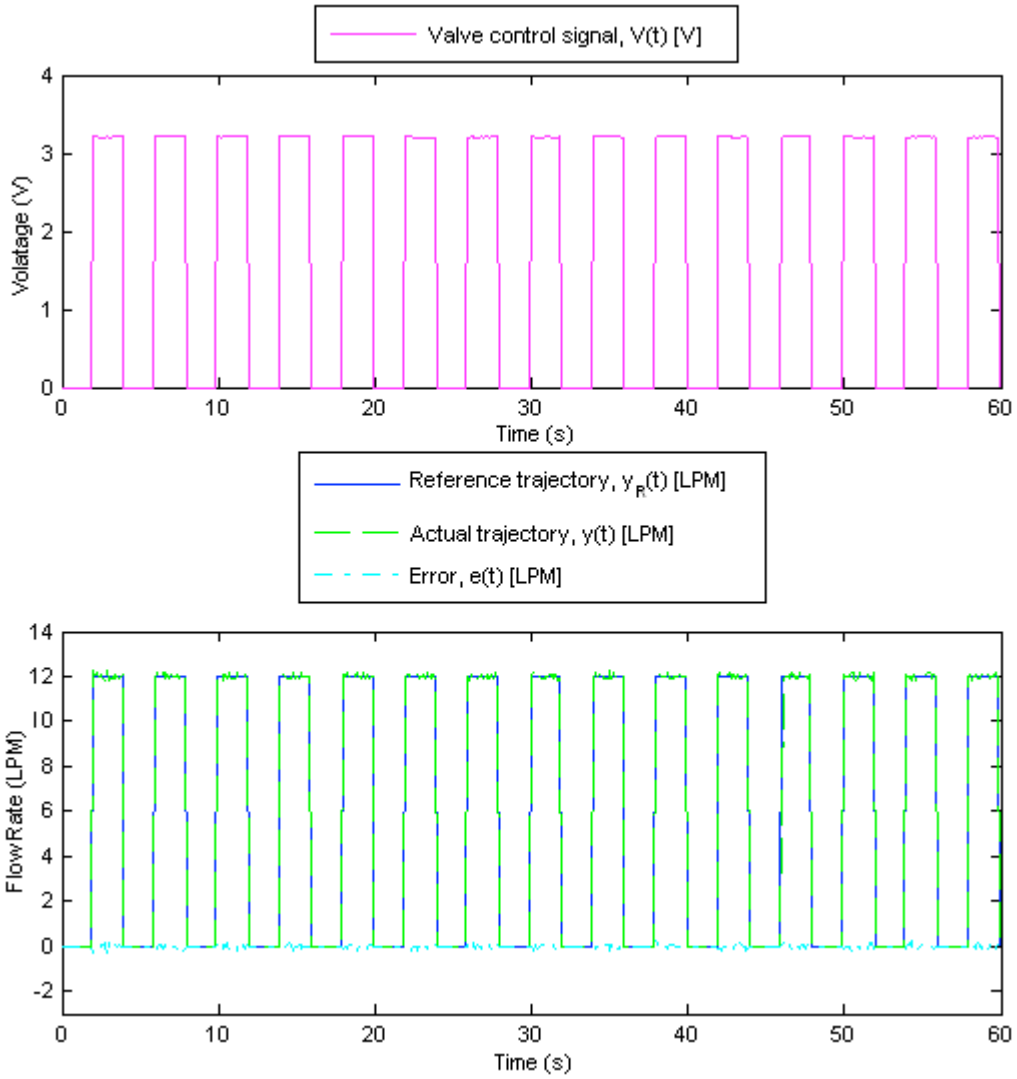

Figure 27 – System response using the adaptive lookup table approach for a periodic input and constant K_f

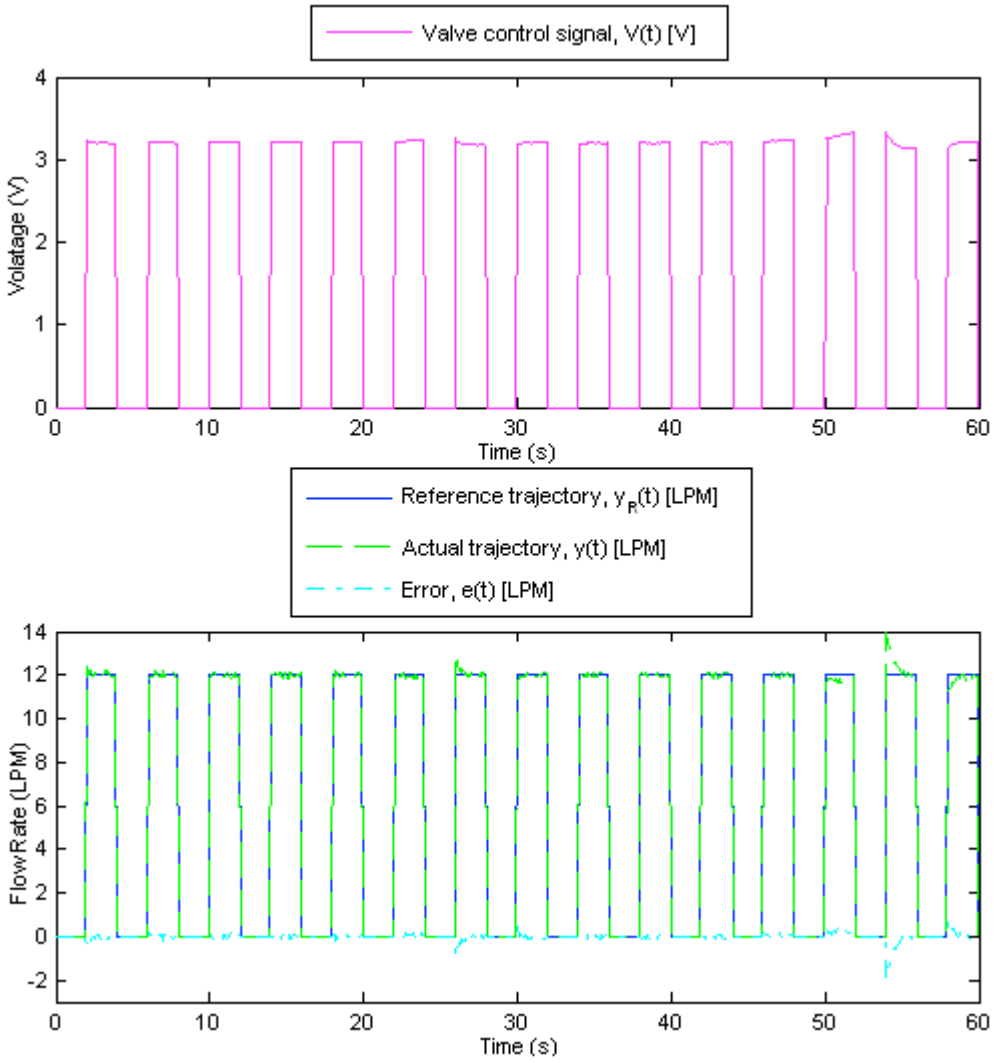

Figure 28 – System response using the adaptive lookup table approach for a periodic input and sawtooth K_f

5.2.3 Recorded Reference

The adaptive lookup table shows exceptional performance in tracking a recorded input. With a sawtooth flow resistance, the control signal is slightly higher than for a constant flow resistance, as expected.

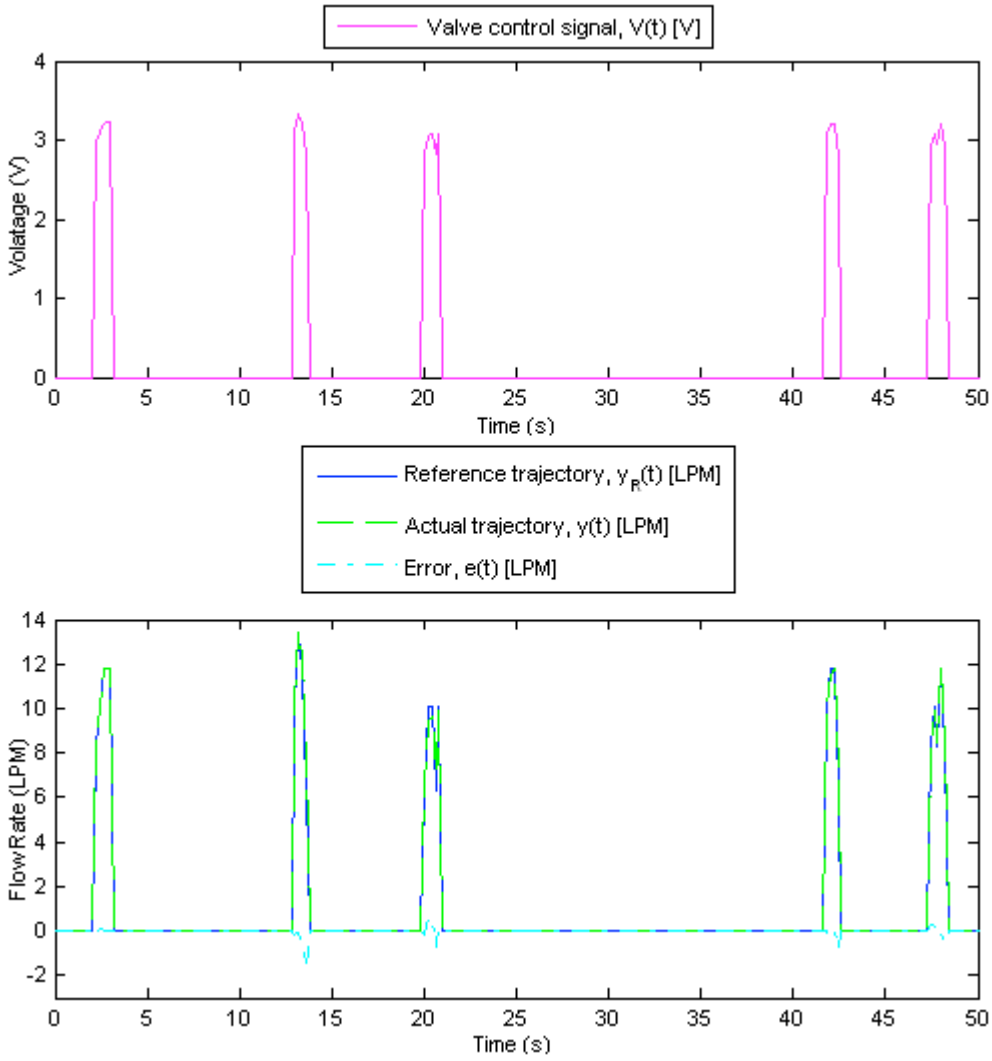

Figure 29 – System response using the adaptive lookup table approach for a recorded input and constant K_f

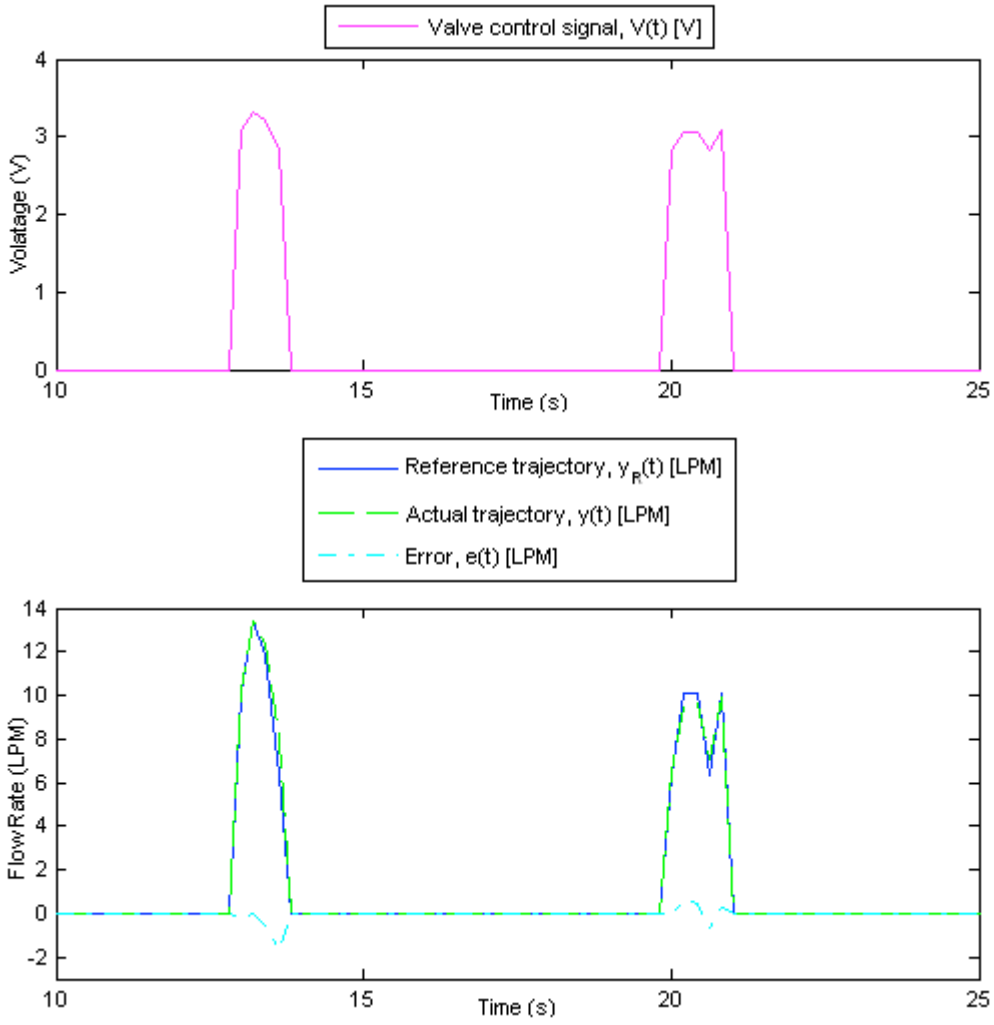

Figure 30 – Two-puff snapshot of the system response using the adaptive lookup table approach for a recorded input and constant K_f

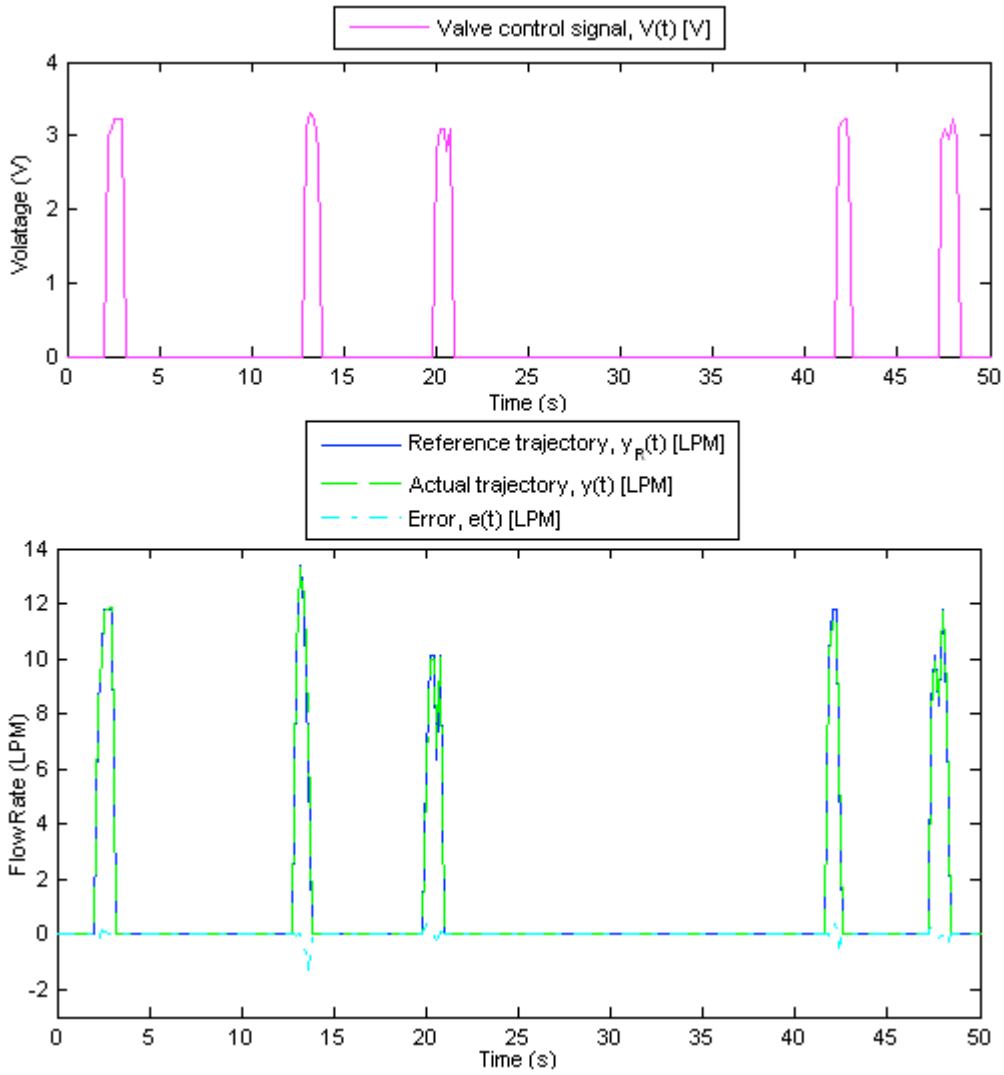

Figure 31 – System response using the adaptive lookup table approach for a recorded input and sawtooth K_f

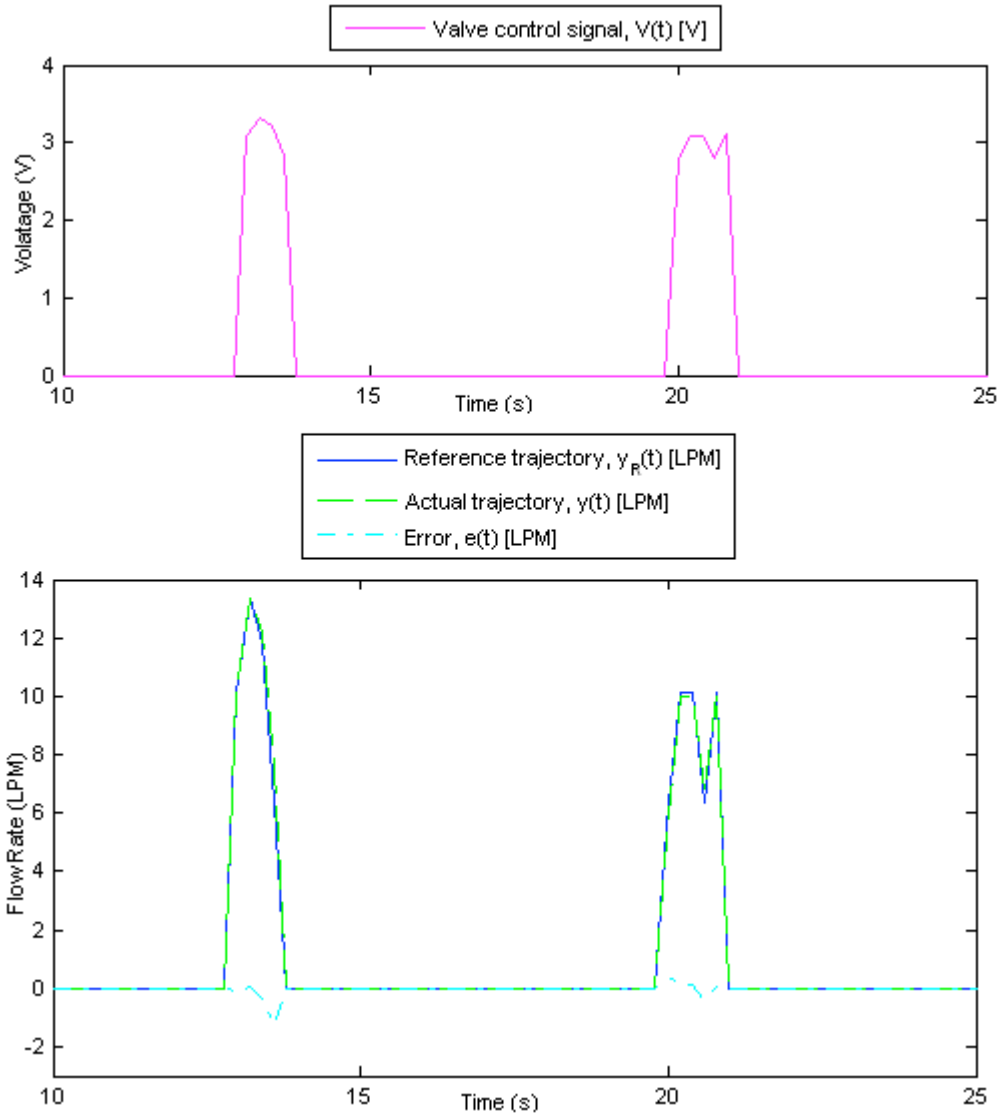

Figure 32 – Two-puff snapshot of the system response using the adaptive lookup table approach for a recorded input and sawtooth K_f

5.3 Performance Comparison

This section will compare the performance of the two controllers by analyzing the following performance measures:

- Percentage error in total volume
- Average percentage error in puff volume

- Regulation of the error

We will also discuss the implementation complexity and practicality of each approach.

	Average Error/Standard Deviation in Puff Volume (%)				Error in Total Volume (%)	
	FL Controller		Adaptive Lookup Table		FL Controller	Adaptive Lookup Table
Step Input						
Constant K_f	-	-	-	-	2.12	0.02
Sawtooth K_f	-	-	-	-	6.88	0.71
Periodic Input						
Constant K_f	3.11	2.49	0.04	0.15	2.22	0.30
Sawtooth K_f	2.96	2.50	0.05	1.23	2.12	0.34
Recorded Input						
Constant K_f	3.15	3.82	1.35	2.67	1.30	0.56
Sawtooth K_f	3.89	3.05	0.66	1.94	1.62	0.28

Figure 33 – Errors in total volume and in puff volume generated by the two controllers in different scenarios

Figure 33 reveals that the error in total volume and the average error in puff volume, in all scenarios were less using the adaptive lookup table approach. While still small, the percentage error in the total volume generated by the feedback linearizing controller is not acceptable for the sensitive application of smoke toxicology studies. Moreover, the average error and standard deviation in puff volume is significantly higher by the feedback linearizing approach.

In tracking a recoded input, the adaptive lookup table generated a larger error than expected. Nonetheless, based on the results in [9], a reasonable percentage error is in the vicinity of 1%.

The reactions of both controllers to a varying flow resistance rendered slightly higher errors in some cases.

Figures 34 to 36 highlight the differences in the error dynamics of the two strategies. The adaptive lookup table approach is an iterative one, and the error does not exhibit as much transient behavior as the more asymptotic-like feedback linearizing approach does. In terms of regulating the error, the feedback linearizing controller did not perform as well. It exhibited large spikes in its transient response and was slow to track the reference.

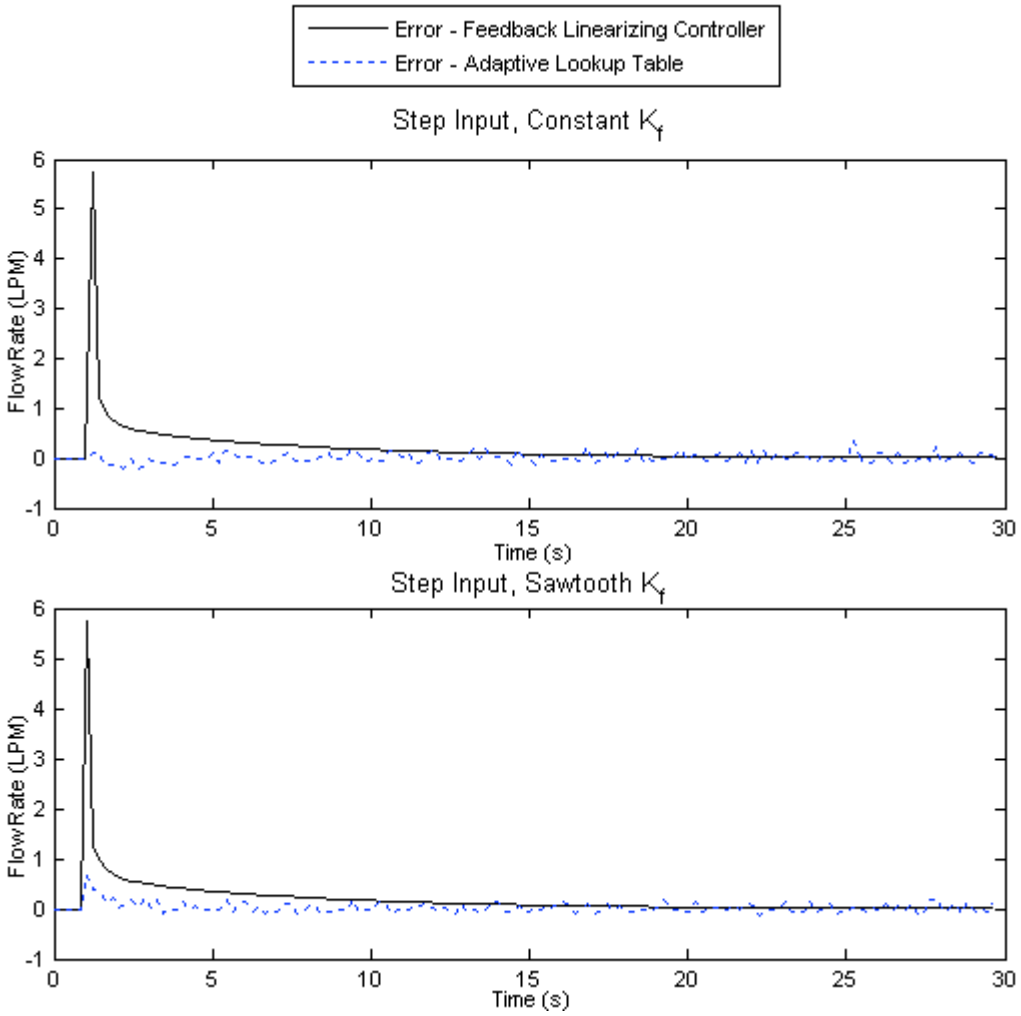

Figure 34 – Errors using the two controllers for a step input

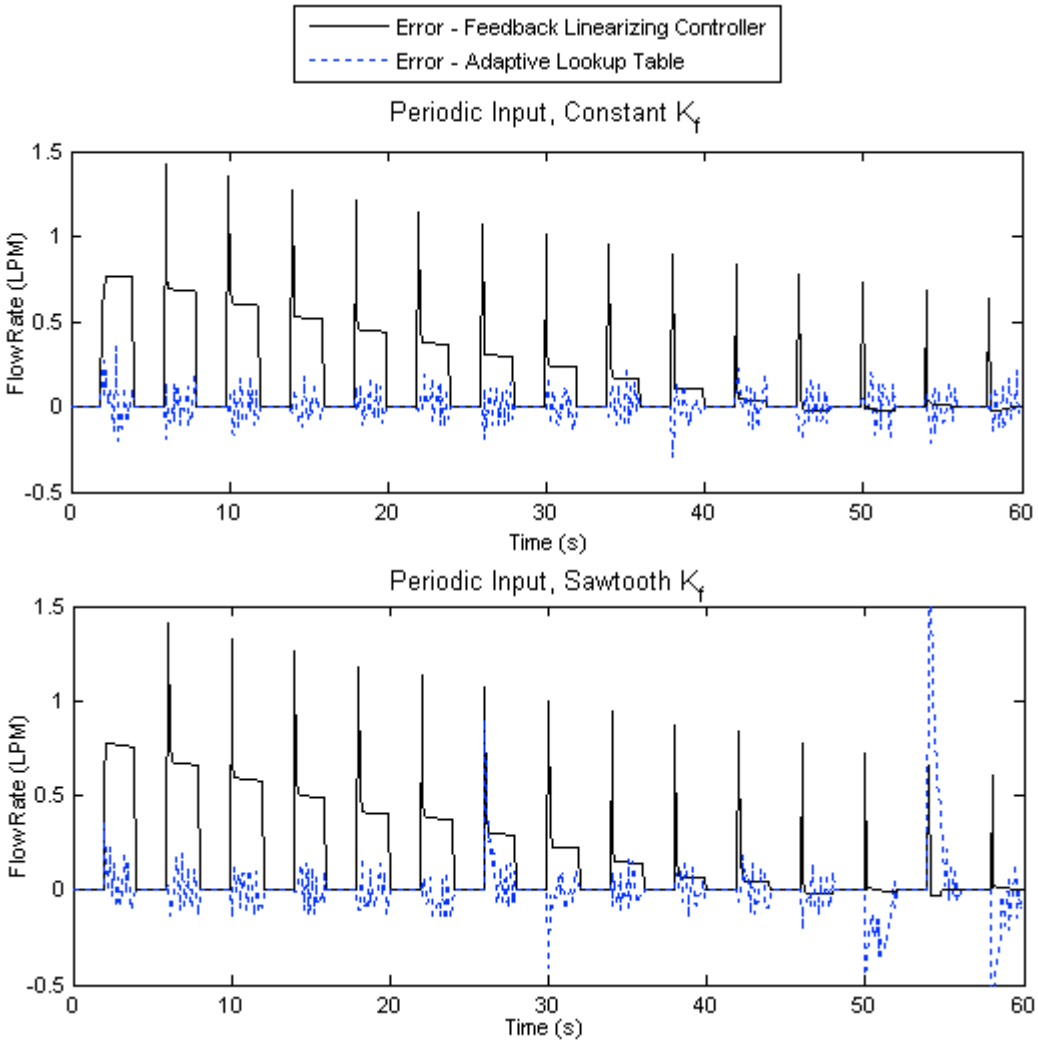

Figure 35 – Errors using the two controllers for a periodic input

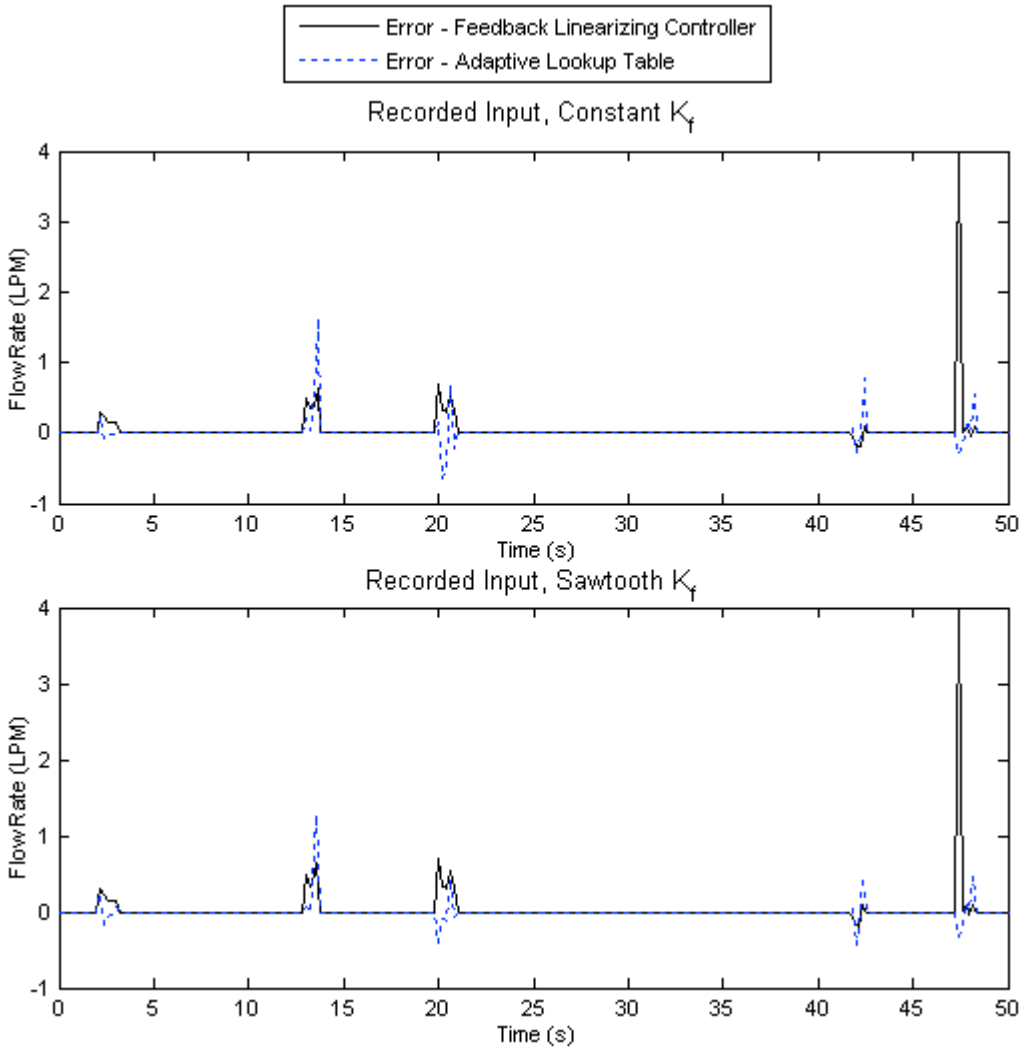

Figure 36 – Errors using the two controllers for a recorded input

Each approach has advantages over the other. The adaptive lookup table has a fairly fine representation of the input-output map of the traversed flow rates in real-time. Since, the adaptive lookup table corrects itself based on experiment history, its map is not comprehensive of all the system dynamics. Therefore, when it is faced with a large change in flow dynamics, it initially computes the control signal based on much older data, until it traverses those points and is given the chance to correct the input-output map.

On the other hand, the feedback linearizing controller is equipped with a substantial set of parameters and knows how the flow resistance is varying at each time step, whereas the adaptive lookup table relies purely on measurements.

5.4 Conclusion

This chapter has provided a comparison of the two flow control strategies that were developed throughout the thesis. A number of scenarios were considered in studying their performance and practicality in implementation.

Chapter 6

Conclusion

This thesis has compared two flow control strategies, a feedback linearizing controller and an adaptive lookup table, to address the need for a new generation smoking machine. This machine goes beyond reducing smoking patterns to an averaged periodic regime, to reproducing actual recorded smoking patterns. The over and underestimation of tobacco smoke components mislead the public and researchers alike.

From a controls perspective, the feedback linearzing controller contributes deeper insight to the problem despite its lower performance with respect to the adaptive lookup table. The feedback linearizing controller showed slow convergence to the reference trajectory, and a future improvement could be to explore other control laws. For instance, retaining the nonlinear term $\frac{Kf}{\rho AL} x_2^2$ may speed up the regulation of the error. Also, since the PI gains needed to be tuned according to the reference trajectory, and so perhaps a gain scheduling scheme can be implemented.

From the operator's perspective, however, the adaptive lookup table provides ease of use, flexibility, and reasonable performance. In terms of practicality and complexity in implementation, we must keep the operator in mind. The end user of a smoking machine is rarely a controls engineer, meaning it is essential to have the ability to make modifications to the physical setup without redefining too many parameters.

This flexibility is offered by the adaptive lookup table because changes in the tubing length, filter type, filter arrangement, and so on, must be determined and fed into the theoretical model of the system and in turn the feedback linearizing controller. By contrast, the adaptive lookup table takes these changes into account during calibration. Although the comparison can be made from different perspectives, the approach that best combines performance with practicality for smoking machines is the adaptive lookup table.

References

[1] Giles, Ranald V., Jack B. Evett, Cheng Liu. *Schaum's Outline of Theory and Problems of Fluid Mechanics and Hyrdaulics*. 3rd Edition. Schaum's Outline Series. McGraw-Hill, Inc. 1994.

[2] Griffiths, Roland and Jack Henningfield. "Experimental analysis of human cigarette smoking behavior." Federation Proceedings. 41 (1982): 234-240.

[3] Griffiths, Roland. "A simple machine for smoke analytical studies and total particulate matter collection for biological studies." Toxicology. 33 (1984): 33-41.

[4] Han, Anne. "Challenging public health acceptability of current international standards on tobacco products: paving the way for strengthened cooperation." Tobacco Control. 10 (2001):105-107.

[5] Jarvis, Martin, Richard Boreham, Paola Primatesta, Colin Feyerabend, and Andrew Bryant. "Nicotine Yield from Machine-Smoked Cigarettes and Nicotine Intakes in Smokers: Evidence from a Representative Population Survey." Journal of the National Cancer Institute. 93 (2001): 134-138.

[6] Khalil, Hassan. Nonlinear Systems. 3rd Edition. Prentice Hall, NJ. 2002.

[7] Mathworks. "Adaptive Lookup Tables." Accessed on 03 January 2006. http://www.mathworks.com/access/helpdesk/help/toolbox/slestim/adaptive.html>

[8] Schaschke, Carl. *Fluid mechanics. Worked examples for engineers.* Institution of Chemical Engineers, UK. 1998.

[9] Shihadeh, Alan and Sima Azar. "A closed-loop control 'playback' smoking machine for generating mainstream smoke aerosols." Journal of Aerosol Medicine. VOL. DATE.

[10] Shihadeh, Alan, Rawad Saleh. "Polycyclic aromatic hydrocarbons, carbon monoxide, "tar", and nicotine in the mainstream smoke aerosol of the narghile water pipe." Food and Chemical Toxicology. 43 (2005). Issue 5.

[11] Shihadeh, Alan, Sima Azar, Charbel Antonios, and Antoine Haddad. "Towards a topographical model of narghile water-pipe café smoking: a pilot study in a high socioeconomic status neighborhood of Beirut, Lebanon." Pharmacology, Biochemistry and Behavior. 79 (2004): 75-82.

[12] White, Frank M. *Fluid Mechanics*. 2nd Edition. McGraw-Hill Book Company. 1986.

[13] Wikipedia. "Hookah." 23 December 2005. Accessed on 28 December 2005. <http://en.wikipedia.org/wiki/Hookah>.

[14] World Health Organization. "Final Report: Advancing Knowledge on Regulating Tobacco Products." Oslo, Norway, 9-11 February 2000.